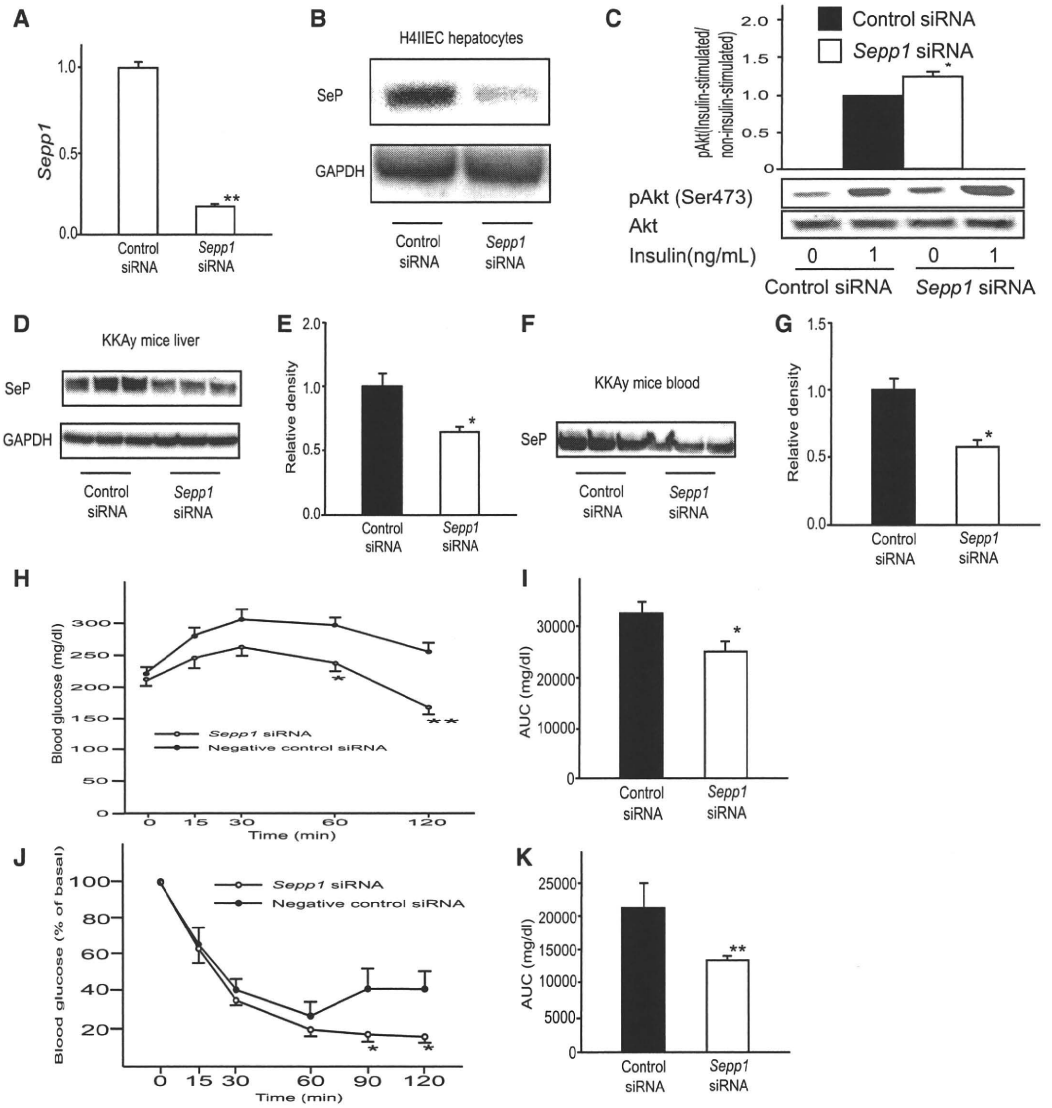

Figure 4. *Sepp1* Knockdown in the Liver Improves Insulin Sensitivity

(A) *Sepp1* mRNA levels in H4IIEC hepatocytes transfected with control or *Sepp1*-specific siRNA (n = 4).

(B) SeP protein production in H4IIEC hepatocytes transfected with *Sepp1*-specific siRNA. SeP production was detected in whole cell lysates by western blotting.

(C) Effects of SeP knockdown on insulin-stimulated serine phosphorylation of Akt in H4IIEC hepatocytes. Data represent the mean ± SEM of three independent experiments.

(D and E) Liver SeP production in KKAy mice injected with control or *Sepp1*-specific siRNA (n = 6). SeP protein levels were measured by western blotting 4 days after injection of siRNA.

(F and G) Blood SeP levels in KKAy mice injected with siRNA. Blood samples were obtained 4 days after siRNA injection (n = 6).

(H–K) Intraperitoneal glucose (H and I) and insulin (J and K) tolerance tests in KKAy mice (n = 6–8) injected with control or *Sepp1*-specific siRNA. Glucose and insulin was administered at doses of 0.3 g/kg body weight and 4 units/kg body weight, respectively.

Area under the curve (AUC) for blood glucose levels is shown in (I) and (K). Data in (A) represent the means ± SEM from four cells per group, and data in (E) and (G)–(K) represent the means ± SEM from six to eight mice per group. *$p < 0.05$ versus cells transfected with control siRNA in (A) and (C). *$p < 0.05$, **$p < 0.01$ versus mice injected with control siRNA in (E) and (G)–(K). See also Figure S2.

rats have been established as an animal model of obesity-related type 2 diabetes (Kawano et al., 1992). Female KKAy mice were obtained from CLEA Japan (Tokyo, Japan). All animals were housed in a 12 hr light/dark cycle and allowed free access to food and water. High-fat and high-sucrose diet (D03062301) was purchased from Research Diets (New Brunswick, NJ). The experiments with OLETF and LETO rats were performed with frozen blood and liver samples obtained in our previous study (Ota et al., 2007).

Purification of SeP

SeP was purified from human plasma via conventional chromatographic methods, as previously described (Saito et al., 1999; Saito and Takahashi, 2002). Homogeneity of purified human SeP was confirmed by analysis of both amino acid composition and sequence (Saito et al., 1999). Concentrations of purified SeP were measured by the Bradford method, using bovine immunoglobulin G as a standard.

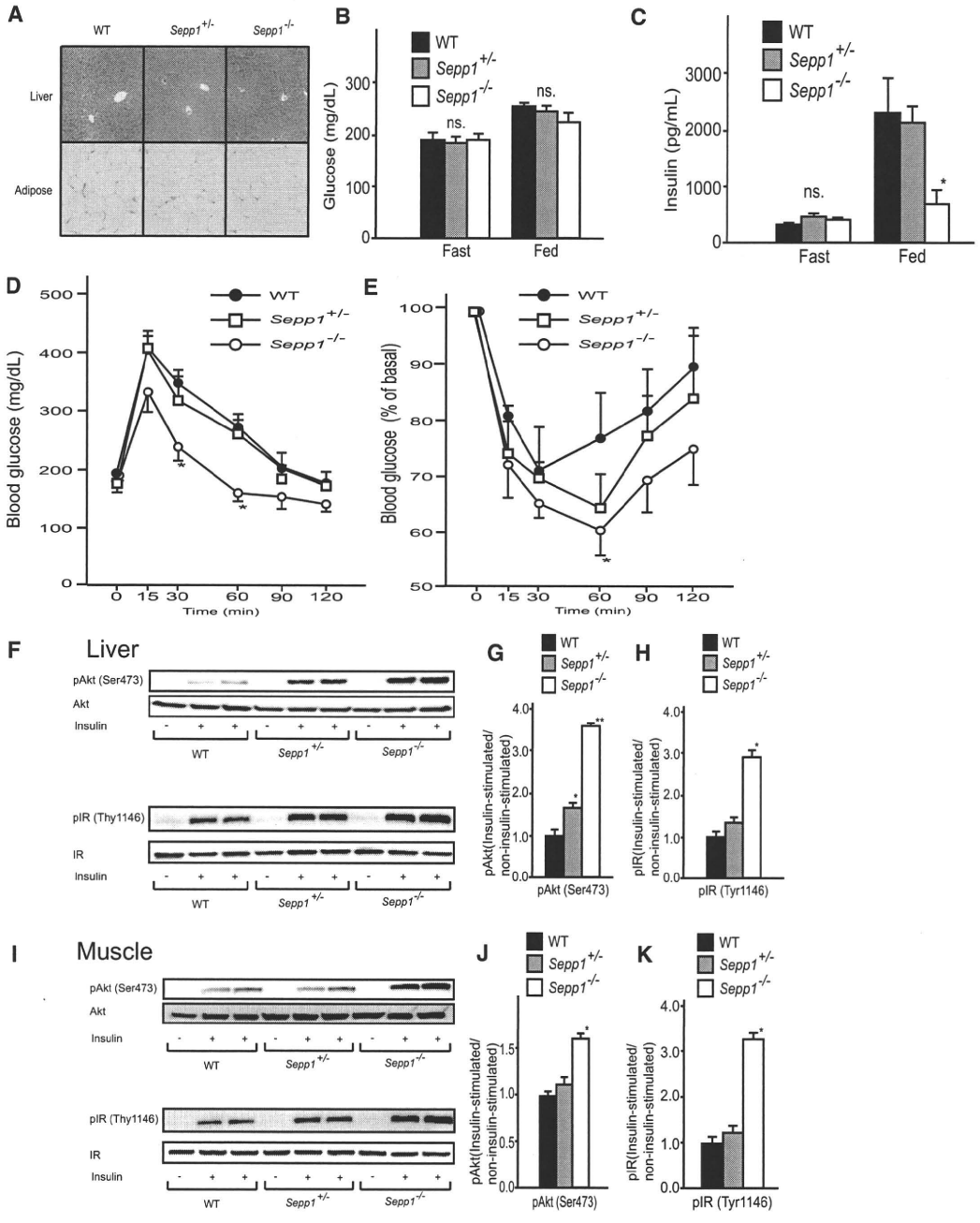

Figure 5. *Sepp1*-Deficient Mice Show Improved Glucose Tolerance and Enhanced Insulin Sensitivity

(A) Hematoxylin-and-eosin-stained liver and epididymal fat sections from male *Sepp1*$^{+/-}$ and *Sepp1*$^{-/-}$ mice.

(B) Blood glucose levels in *Sepp1*-deficient mice (n = 7). The mice were fasted for 6 hr.

(C) Blood insulin levels in *Sepp1*-deficient mice (n = 7).

(D and E) Intraperitoneal glucose (D) and insulin (E) tolerance tests in male *Sepp1*-deficient mice (n = 7). Glucose and insulin were administered at doses of 1.5 g/kg body weight and 4 units/kg body weight, respectively.

(F–K) Western blot analysis of phosphorylated Akt (pAkt) and phosphorylated insulin receptor (pIR) in liver (F–H) and skeletal muscle (I–K). Mice (n = 6) were stimulated with insulin (administered intraperitoneally). At 20 min after insulin stimulation, mice were anesthetized, and liver and hind-limb muscle samples removed for analysis.

Data in (B)–(E), (G), (H), (J), and (K) represent the means ± SEM from six to seven mice per group. *$p < 0.05$, **$p < 0.01$ versus wild-type mice. See also Figure S3.

siRNA Injection into KKAy mice

Delivery of siRNA targeted to the liver was performed by tail vein injections into mice, via hydrodynamic techniques, as previously described (McCaffrey et al., 2002; Zender et al., 2003). For these experiments, KKAy mice at 7–8 weeks of age (31–33 g body weight) were used. Mice were anesthetized with pentobarbital, and 2 nmol of siRNA, diluted in 3 ml of PBS, was injected into the tail vein over 15–20 s. All siRNAs were purchased from Applied Biosystems (Silencer^{R} In Vivo Ready Pre-designed siRNA). *Sepp1* siRNAs with the following

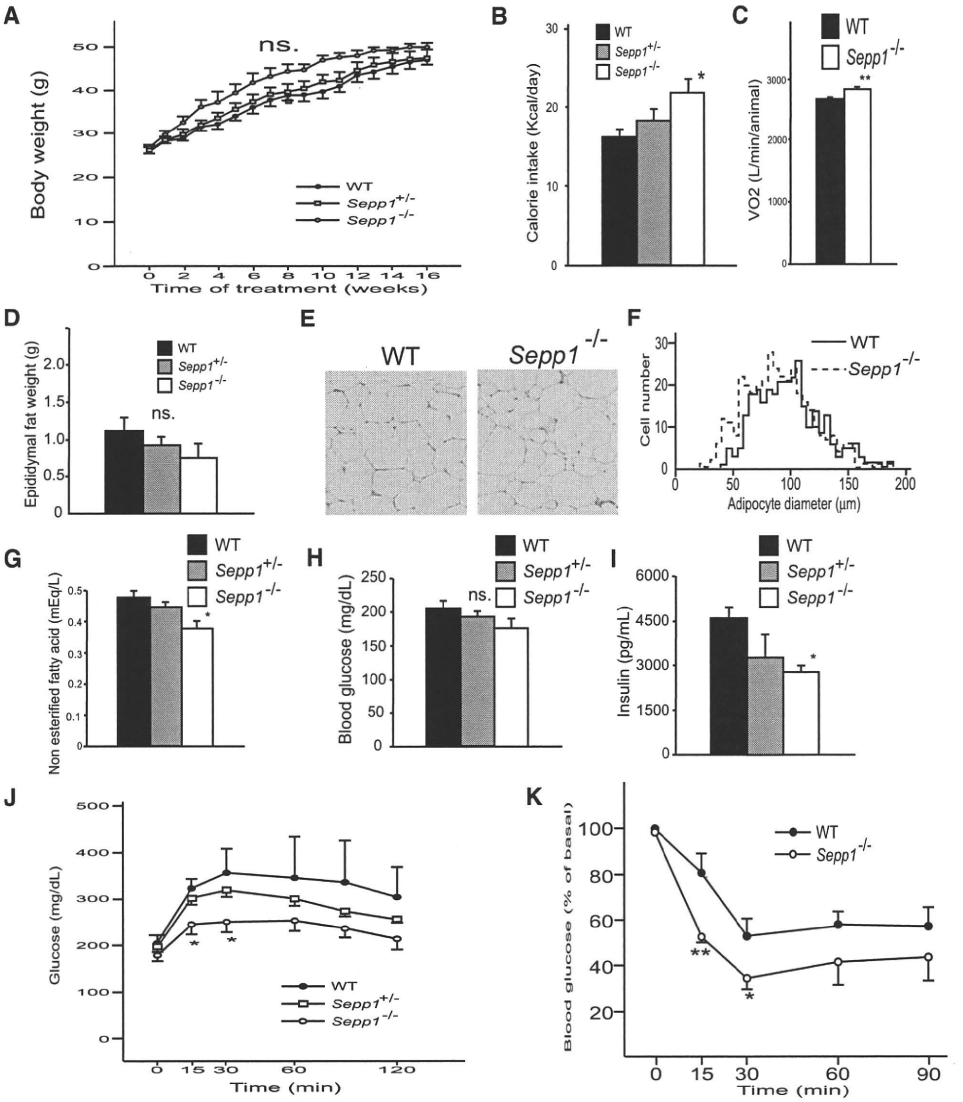

Figure 6. *Sepp1*-Deficient Mice Are Protected from Diet-Induced Insulin Resistance and Adipocyte Hypertrophy

(A) Body weight of *Sepp1*-deficient and wild-type mice fed a high-fat, high-sucrose diet (HFHSD; n = 4–8). Sixteen-week-old male mice were fed a HFHSD for 16 weeks.

(B) Daily calorie intake in *Sepp1*-deficient and wild-type mice (n = 4–8).

(C) Energy expenditure (as measured by VO_2 consumption through indirect calorimetry; n = 4).

(D) Epididymal fat mass in *Sepp1*-deficient and wild-type mice fed HFHSD (n = 4–7).

(E) Hematoxylin-and-eosin-stained epididymal fat sections from wild-type and *Sepp1*$^{-/-}$ mice.

(F) Histogram showing adipocyte diameters. We determined adipocyte diameters by measuring at least 300 adipocytes randomly selected from four independent sections.

(G) Blood nonestimated fatty acid levels in *Sepp1*-deficient and wild-type mice fed HFHSD (n = 4–7).

(H) Blood glucose levels in *Sepp1*-deficient and wild-type mice fed HFHSD (n = 4–8).

(I) Blood insulin levels in *Sepp1*-deficient and wild-type mice fed HFHSD (n = 4–8). Blood samples were obtained from mice fed a HFHSD for 16 weeks after a 12 hr fast in (G)–(I).

(J) Intraperitoneal glucose tolerance tests in wild-type and *Sepp1*-deficient mice (n = 4–8). Glucose was administered at a dose of 0.3 g/kg body weight.

(K) Intraperitoneal insulin tolerance tests in wild-type and *Sepp1*-deficient mice (n = 5–10). Insulin was administered at a dose of 2.0 units/kg body weight.

Data in (A)–(D) and (G)–(K) represent the means ± SEM from four to ten mice per group. *$p < 0.05$, **$p < 0.01$ versus wild-type mice. See also Figure S4.

sequence were synthesized: mouse *Sepp1*, 5′-GGUGUCAGAACACAUC GCAtt-3′ (sense). Negative control siRNA was also used and had no significant homology with any known gene sequences in mouse, rat, or human. Glucose and insulin loading tests were performed 2–7 days after injection of mice with siRNA.

SeP Knockout Mice

SeP knockout mice were produced by homologous recombination with genomic DNA cloned from an Sv-129 P1 library, as described previously (Hill et al., 2003). As female SeP knockout mice had inconsistent phenotypes, only male mice were used in this study.

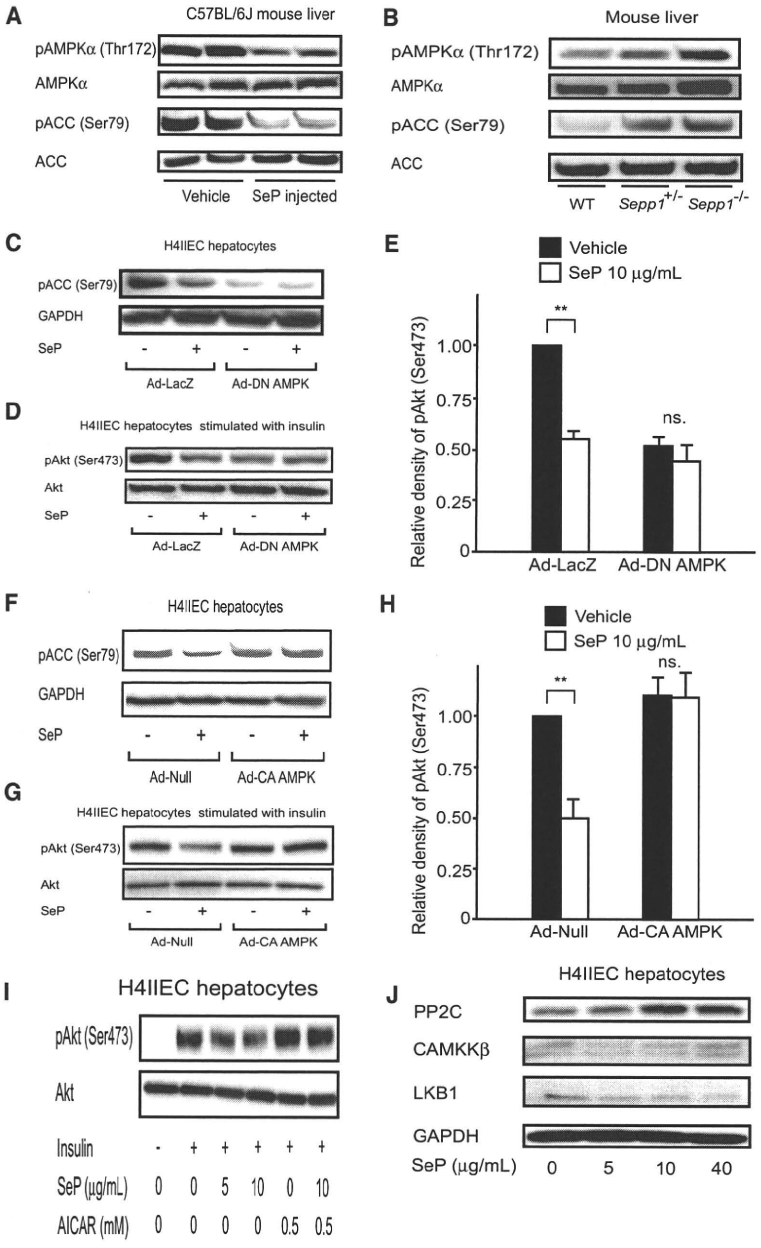

Figure 7. SeP Reduces Phosphorylation of AMPK and ACC in Hepatocytes

(A) Phosphorylation of AMPK and ACC in the liver of mice injected with SeP or vehicle. C57BL/6J mice were injected intravenously with purified human SeP (1 mg/kg body weight) or vehicle (phosphate-buffered saline). At 6 hr after injection, the liver was removed.

(B) Phosphorylation of AMPK and ACC in the liver of *Sepp1*-deficient mice after a 12 hr fast.

(C–E) Effects of dominant-negative AMPK on ACC phosphorylation (C) and insulin-stimulated Akt phosphorylation (D and E) in H4IIEC hepatocytes treated with SeP.

(F–H) Effects of constitutively active AMPK on ACC phosphorylation (F) and insulin-stimulated Akt phosphorylation (G and H) in H4IIEC hepatocytes treated with SeP.

(I) Effect of AICAR on SeP-induced insulin resistance in H4IIEC hepatocytes.

(J) Levels of PP2C, CaMKKβ, and LKB1 in H4IIEC hepatocytes treated with various concentrations of SeP for 12 hr.

Data in (E) and (H) represent the means ± SEM from three independent experiments. **p < 0.01 versus vehicle-treated cells. See also Figure S5.

Statistical Analyses

All data were analyzed using the Japanese Windows Edition of the Statistical Package for Social Science (SPSS) Version 11.0. Numeric values are reported as the mean ± SEM. Differences between two groups were assessed with unpaired two-tailed t tests. Data involving more than two groups were assessed by analysis of variance (ANOVA). Glucose and insulin tolerance tests were examined with repeated-measures ANOVA.

ACCESSION NUMBERS

Microarray data have been deposited in Gene Expression Omnibus under accession number GSE23343.

SUPPLEMENTAL INFORMATION

Supplemental Information includes Supplemental Experimental Procedures, five figures, and five tables and can be found with this article online at doi:10.1016/j.cmet.2010.09.015.

ACKNOWLEDGMENTS

We thank Kuniaki Arai of Kanazawa University for liver biopsies and Isao Usui, Hajime Ishihara, and Toshiyasu Sasaoka of Toyama University for supplying their technical expertise on Western blot analyses of phosphoproteins. We thank Yuriko Furuta and Yoko Hashimoto for technical assistance. We thank Fabienne Foufelle of Université Pierre et Marie Curie for providing adenovirus vector encoding DN-AMPK. We are indebted to Kristina E. Hill and Raymond F. Burk of Vanderbilt University School of Medicine for the *Sepp1* knockout mice. This work was supported by Takeda Science Foundation and Grants-in-Aid from the Ministry of Education, Culture, Sports, Science and Technology, Japan. We also thank Cathie Chung for editing the manuscript.

Received: February 2, 2009
Revised: April 29, 2010
Accepted: August 13, 2010
Published: November 2, 2010

REFERENCES

Andoh, A., Hirashima, M., Maeda, H., Hata, K., Inatomi, O., Tsujikawa, T., Sasaki, M., Takahashi, K., and Fujiyama, Y. (2005). Serum selenoprotein-P levels in patients with inflammatory bowel disease. Nutrition *21*, 574–579.

Auberger, P., Falquerho, L., Contreres, J.O., Pages, G., Le Cam, G., Rossi, B., and Le Cam, A. (1989). Characterization of a natural inhibitor of the insulin receptor tyrosine kinase: cDNA cloning, purification, and anti-mitogenic activity. Cell *58*, 631–640.

Bellinger, F.P., He, Q.P., Bellinger, M.T., Lin, Y., Raman, A.V., White, L.R., and Berry, M.J. (2008). Association of selenoprotein p with Alzheimer's pathology in human cortex. J. Alzheimers Dis. *15*, 465–472.

Bleys, J., Navas-Acien, A., and Guallar, E. (2007). Serum selenium and diabetes in U.S. adults. Diabetes Care *30*, 829–834.

Burk, R.F., and Hill, K.E. (2005). Selenoprotein P: an extracellular protein with unique physical characteristics and a role in selenium homeostasis. Annu. Rev. Nutr. *25*, 215–235.

Burk, R.F., Hill, K.E., Olson, G.E., Weeber, E.J., Motley, A.K., Winfrey, V.P., and Austin, L.M. (2007). Deletion of apolipoprotein E receptor-2 in mice lowers brain selenium and causes severe neurological dysfunction and death when a low-selenium diet is fed. J. Neurosci. *27*, 6207–6211.

Carlson, B.A., Novoselov, S.V., Kumaraswamy, E., Lee, B.J., Anver, M.R., Gladyshev, V.N., and Hatfield, D.L. (2004). Specific excision of the selenocysteine tRNA[Ser]Sec (Trsp) gene in mouse liver demonstrates an essential role of selenoproteins in liver function. J. Biol. Chem. *279*, 8011–8017.

Davies, S.P., Helps, N.R., Cohen, P.T., and Hardie, D.G. (1995). 5′-AMP inhibits dephosphorylation, as well as promoting phosphorylation, of the AMP-activated protein kinase. Studies using bacterially expressed human protein phosphatase-2C alpha and native bovine protein phosphatase-2AC. FEBS Lett. *377*, 421–425.

Després, J.P., Lamarche, B., Mauriège, P., Cantin, B., Dagenais, G.R., Moorjani, S., and Lupien, P.J. (1996). Hyperinsulinemia as an independent risk factor for ischemic heart disease. N. Engl. J. Med. *334*, 952–957.

Friedman, J.M., and Halaas, J.L. (1998). Leptin and the regulation of body weight in mammals. Nature *395*, 763–770.

Hill, K.E., Zhou, J., McMahan, W.J., Motley, A.K., Atkins, J.F., Gesteland, R.F., and Burk, R.F. (2003). Deletion of selenoprotein P alters distribution of selenium in the mouse. J. Biol. Chem. *278*, 13640–13646.

Kahn, B.B., Alquier, T., Carling, D., and Hardie, D.G. (2005). AMP-activated protein kinase: ancient energy gauge provides clues to modern understanding of metabolism. Cell Metab. *1*, 15–25.

Kawano, K., Hirashima, T., Mori, S., Saitoh, Y., Kurosumi, M., and Natori, T. (1992). Spontaneous long-term hyperglycemic rat with diabetic complications. Otsuka Long-Evans Tokushima Fatty (OLETF) strain. Diabetes *41*, 1422–1428.

Maeda, K., Okubo, K., Shimomura, I., Funahashi, T., Matsuzawa, Y., and Matsubara, K. (1996). cDNA cloning and expression of a novel adipose specific collagen-like factor, apM1 (AdiPose Most abundant Gene transcript 1). Biochem. Biophys. Res. Commun. *221*, 286–289.

Maeda, N., Shimomura, I., Kishida, K., Nishizawa, H., Matsuda, M., Nagaretani, H., Furuyama, N., Kondo, H., Takahashi, M., Arita, Y., et al. (2002). Diet-induced insulin resistance in mice lacking adiponectin/ACRP30. Nat. Med. *8*, 731–737.

Masiulis, I., Quill, T.A., Burk, R.F., and Herz, J. (2009). Differential functions of the Apoer2 intracellular domain in selenium uptake and cell signaling. Biol. Chem. *390*, 67–73.

McCaffrey, A.P., Meuse, L., Pham, T.T., Conklin, D.S., Hannon, G.J., and Kay, M.A. (2002). RNA interference in adult mice. Nature *418*, 38–39.

Minokoshi, Y., Kim, Y.B., Peroni, O.D., Fryer, L.G., Müller, C., Carling, D., and Kahn, B.B. (2002). Leptin stimulates fatty-acid oxidation by activating AMP-activated protein kinase. Nature *415*, 339–343.

Misu, H., Takamura, T., Matsuzawa, N., Shimizu, A., Ota, T., Sakurai, M., Ando, H., Arai, K., Yamashita, T., Honda, M., et al. (2007). Genes involved in oxidative phosphorylation are coordinately upregulated with fasting hyperglycaemia in livers of patients with type 2 diabetes. Diabetologia *50*, 268–277.

Oike, Y., Akao, M., Yasunaga, K., Yamauchi, T., Morisada, T., Ito, Y., Urano, T., Kimura, Y., Kubota, Y., Maekawa, H., et al. (2005). Angiopoietin-related growth factor antagonizes obesity and insulin resistance. Nat. Med. *11*, 400–408.

Olson, G.E., Winfrey, V.P., Nagdas, S.K., Hill, K.E., and Burk, R.F. (2007). Apolipoprotein E receptor-2 (ApoER2) mediates selenium uptake from selenoprotein P by the mouse testis. J. Biol. Chem. *282*, 12290–12297.

Ota, T., Takamura, T., Kurita, S., Matsuzawa, N., Kita, Y., Uno, M., Akahori, H., Misu, H., Sakurai, M., Zen, Y., et al. (2007). Insulin resistance accelerates a dietary rat model of nonalcoholic steatohepatitis. Gastroenterology *132*, 282–293.

Persson-Moschos, M., Alfthan, G., and Akesson, B. (1998). Plasma selenoprotein P levels of healthy males in different selenium status after oral supplementation with different forms of selenium. Eur. J. Clin. Nutr. *52*, 363–367.

Saito, Y., and Takahashi, K. (2002). Characterization of selenoprotein P as a selenium supply protein. Eur. J. Biochem. *269*, 5746–5751.

Saito, Y., Hayashi, T., Tanaka, A., Watanabe, Y., Suzuki, M., Saito, E., and Takahashi, K. (1999). Selenoprotein P in human plasma as an extracellular phospholipid hydroperoxide glutathione peroxidase. Isolation and enzymatic characterization of human selenoprotein p. J. Biol. Chem. *274*, 2866–2871.

Saito, Y., Watanabe, Y., Saito, E., Honjoh, T., and Takahashi, K. (2001). Production and application of monoclonal antibodies to human selenoprotein P. J. Health Sci. *47*, 346–352.

Saltiel, A.R., and Kahn, C.R. (2001). Insulin signalling and the regulation of glucose and lipid metabolism. Nature *414*, 799–806.

Scherer, P.E., Williams, S., Fogliano, M., Baldini, G., and Lodish, H.F. (1995). A novel serum protein similar to C1q, produced exclusively in adipocytes. J. Biol. Chem. *270*, 26746–26749.

Schomburg, L., Schweizer, U., Holtmann, B., Flohé, L., Sendtner, M., and Köhrle, J. (2003). Gene disruption discloses role of selenoprotein P in selenium delivery to target tissues. Biochem. J. *370*, 397–402.

Speckmann, B., Walter, P.L., Alili, L., Reinehr, R., Sies, H., Klotz, L.O., and Steinbrenner, H. (2008). Selenoprotein P expression is controlled through interaction of the coactivator PGC-1alpha with FoxO1a and hepatocyte nuclear factor 4alpha transcription factors. Hepatology *48*, 1998–2006.

Srinivas, P.R., Wagner, A.S., Reddy, L.V., Deutsch, D.D., Leon, M.A., Goustin, A.S., and Grunberger, G. (1993). Serum alpha 2-HS-glycoprotein is an inhibitor of the human insulin receptor at the tyrosine kinase level. Mol. Endocrinol. *7*, 1445–1455.

Steinberg, G.R., Michell, B.J., van Denderen, B.J., Watt, M.J., Carey, A.L., Fam, B.C., Andrikopoulos, S., Proietto, J., Görgün, C.Z., Carling, D., et al. (2006). Tumor necrosis factor alpha-induced skeletal muscle insulin resistance involves suppression of AMP-kinase signaling. Cell Metab. *4*, 465–474.

Steppan, C.M., Bailey, S.T., Bhat, S., Brown, E.J., Banerjee, R.R., Wright, C.M., Patel, H.R., Ahima, R.S., and Lazar, M.A. (2001). The hormone resistin links obesity to diabetes. Nature *409*, 307–312.

Takamura, T., Sakurai, M., Ota, T., Ando, H., Honda, M., and Kaneko, S. (2004). Genes for systemic vascular complications are differentially expressed in the livers of type 2 diabetic patients. Diabetologia *47*, 638–647.

Takeda, S., Sato, N., Uchio-Yamada, K., Sawada, K., Kunieda, T., Takeuchi, D., Kurinami, H., Shinohara, M., Rakugi, H., and Morishita, R. (2010). Diabetes-accelerated memory dysfunction via cerebrovascular inflammation and Abeta deposition in an Alzheimer mouse model with diabetes. Proc. Natl. Acad. Sci. USA *107*, 7036–7041.

Takeshita, Y., Takamura, T., Hamaguchi, E., Shimizu, A., Ota, T., Sakurai, M., and Kaneko, S. (2006). Tumor necrosis factor-alpha-induced production of plasminogen activator inhibitor 1 and its regulation by pioglitazone and cerivastatin in a nonmalignant human hepatocyte cell line. Metabolism *55*, 1464–1472.

Velculescu, V.E., Zhang, L., Vogelstein, B., and Kinzler, K.W. (1995). Serial analysis of gene expression. Science *270*, 484–487.

Walter, P.L., Steinbrenner, H., Barthel, A., and Klotz, L.O. (2008). Stimulation of selenoprotein P promoter activity in hepatoma cells by FoxO1a transcription factor. Biochem. Biophys. Res. Commun. *365*, 316–321.

Xu, A., Lam, M.C., Chan, K.W., Wang, Y., Zhang, J., Hoo, R.L., Xu, J.Y., Chen, B., Chow, W.S., Tso, A.W., and Lam, K.S. (2005). Angiopoietin-like protein 4 decreases blood glucose and improves glucose tolerance but induces hyperlipidemia and hepatic steatosis in mice. Proc. Natl. Acad. Sci. USA *102*, 6086–6091.

Yamauchi, T., Kamon, J., Minokoshi, Y., Ito, Y., Waki, H., Uchida, S., Yamashita, S., Noda, M., Kita, S., Ueki, K., et al. (2002). Adiponectin stimulates glucose utilization and fatty-acid oxidation by activating AMP-activated protein kinase. Nat. Med. *8*, 1288–1295.

Yang, Q., Graham, T.E., Mody, N., Preitner, F., Peroni, O.D., Zabolotny, J.M., Kotani, K., Quadro, L., and Kahn, B.B. (2005). Serum retinol binding protein 4 contributes to insulin resistance in obesity and type 2 diabetes. Nature *436*, 356–362.

Zender, L., Hutker, S., Liedtke, C., Tillmann, H.L., Zender, S., Mundt, B., Waltemathe, M., Gosling, T., Flemming, P., Malek, N.P., et al. (2003). Caspase 8 small interfering RNA prevents acute liver failure in mice. Proc. Natl. Acad. Sci. USA *100*, 7797–7802.

Histological Course of Nonalcoholic Fatty Liver Disease in Japanese Patients

Tight glycemic control, rather than weight reduction, ameliorates liver fibrosis

ERIKA HAMAGUCHI, MD, PHD[1]
TOSHINARI TAKAMURA, MD, PHD[1]
MASARU SAKURAI, MD, PHD[2]
EISHIRO MIZUKOSHI, MD, PHD[3]
YOH ZEN, MD, PHD[4]
YUMIE TAKESHITA, MD, PHD[1]
SEIICHIRO KURITA, MD, PHD[1]
KUNIAKI ARAI, MD, PHD[3]
TATSUYA YAMASHITA, MD, PHD[3]
MOTOKO SASAKI, MD, PHD[5]
YASUNI NAKANUMA, MD, PHD[5]
SHUICHI KANEKO, MD, PHD[3]

OBJECTIVE — The goal of this study was to examine whether metabolic abnormalities are responsible for the histological changes observed in Japanese patients with nonalcoholic fatty liver disease (NAFLD) who have undergone serial liver biopsies.

RESEARCH DESIGN AND METHODS — In total, 39 patients had undergone consecutive liver biopsies. Changes in their clinical data were analyzed, and biopsy specimens were scored histologically for stage.

RESULTS — The median follow-up time was 2.4 years (range 1.0–8.5). Liver fibrosis had improved in 12 patients (30.7%), progressed in 11 patients (28.2%), and remained unchanged in 16 patients (41%). In a Cox proportional hazard model, decrease in A1C and use of insulin were associated with improvement of liver fibrosis independent of age, sex, and BMI. However, ΔA1C was more strongly associated with the improvement of liver fibrosis than use of insulin after adjustment for each other (χ^2; 7.97 vs. 4.58, respectively).

CONCLUSIONS — Tight glycemic control may prevent histological progression in Japanese patients with NAFLD.

Diabetes Care 33:284–286, 2010

Accumulating trans-sectional evidence suggests that the presence of multiple metabolic disorders, including obesity, diabetes, dyslipidemia, hypertension, and ultimately metabolic syndrome, are associated with nonalcoholic fatty liver disease (NAFLD) (1). However, it remains unclear which metabolic abnormalities are responsible for the pathological progression of NAFLD, especially in Japanese patients, who generally are not severely obese compared with Western patients.

We retrospectively compared clinical features with the histological changes in the livers of Japanese patients with NAFLD who had undergone serial liver biopsies.

RESEARCH DESIGN AND METHODS

— We recruited 195 patients with clinically suspected NAFLD who had undergone liver biopsies at Kanazawa University Hospital from 1997 through 2008. For details about the study subjects and the exclusion criteria, see supplementary Fig. 1 in the online appendix, available at http://care.diabetesjournals.org/cgi/content/full/dc09-0148/DC1. Of 178 patients diagnosed histologically as having NAFLD, 39 had undergone serial liver biopsies.

Data collection

Clinical information, including age, sex, body measurements, and prevalence of metabolic abnormalities, was obtained for each patient. Venous blood samples drawn for laboratory testing before the liver biopsies were obtained. All subjects had been administered a 75-g oral glucose tolerance test at baseline and at follow-up.

Liver biopsies

Biopsies were obtained after a thorough clinical evaluation and receipt of signed informed consent from each patient. All biopsies were analyzed twice and at separate times randomly by a single pathologist who was blinded to the clinical information and the order in which the biopsies were obtained. The biopsied tissues were scored for steatosis, stage, and grade as described (2), according to the standard criteria for grading and staging of nonalcoholic steatohepatitis proposed by Brunt et al. (3).

For additional details on subjects, data collection methods, liver pathology, and statistical analyses, see supplementary Methods in the online appendix.

RESULTS

— The basal clinical and biochemical data from 39 patients with NAFLD are described in supplementary Table 1. Prevalence of type 2 diabetes, hypertension, and dyslipidemia were 77, 36, and 64%, respectively. The median follow-up period was 2.4 years (range 1.0–8.5). Medications for diabetes and medication changes during the follow-up period are described in supplementary Table 2. Seventeen patients treated with oral diabetic agents were switched to insulin therapy after the initial biopsy. No patients initiated pioglitazone during follow-up.

From the [1]Department of Disease Control and Homeostasis, Kanazawa University Graduate School of Medical Science, Ishikawa, Japan; the [2]Department of Epidemiology and Public Health, Kanazawa Medical University, Ishikawa, Japan; the [3]Department of Gastroenterology, Kanazawa University Hospital, Ishikawa, Japan; the [4]Division of Pathology, Kanazawa University Hospital, Ishikawa, Japan; and the [5]Department of Human Pathology, Kanazawa University Graduate School of Medical Science, Ishikawa, Japan.
Corresponding author: Toshinari Takamura, ttakamura@m-kanazawa.jp.
Received 8 February 2009 and accepted 20 October 2009. Published ahead of print at http://care.diabetesjournals.org on 30 October 2009. DOI: 10.2337/dc09-0148.

Table 1—*Baseline and follow-up clinical features and gradients of laboratory markers associated with changes in liver fibrosis in 39 patients with NAFLD*

	Baseline				Follow-up			
	Improved	Stable	Progressed	*P*	Improved	Stable	Progressed	*P*
n	12	16	11		12	16	11	—
Simple fatty liver:nonalcoholic steatohepatitis (*n*)	3:9	9:7	10:1		10:2	9:7	6:5	
Age (years)	51.5 (29–66)	48.5 (20–79)	51.5 (29–66)	0.97				
Sex (M:F)	5:7	12:4	5:7	0.17				
BMI (kg/m^2)	27.5 (23.2–34.1)	27.7 (22.5–44.4)	30.9 (23.4–37.7)	0.74	26.9 (22.8–31.2)	29.1 (24.3–44.8)	30.7 (24.1–36.3)	0.13
Aspartate transaminase (IU/l)	70 (11–106)	29 (14–86)	32 (13–83)	0.05	23 (11–28)	26 (15–71)	24 (14–164)	0.20
Alanine transaminase (IU/l)	71 (10–209)	48 (23–81)	40 (11–162)	0.13	21 (11–53)	36 (21–66)	31 (12–202)	0.10
Fasting plasma glucose (mg/dl)	133 (96–207)	143 (87–414)	111 (76–167)	0.20	103 (93–220)	121 (83–198)	116 (88–199)	0.51
A1C (%)	8.2 (4.7–11.6)	8.0 (4.9–13.6)	6.2 (5.1–9.5)	0.27	6.0 (5.0–9.0)	6.2 (5.0–10.0)	7.0 (6.0–11.0)	0.10
HOMA-IR	3.9 (0.7–5.5)	3.4 (1.9–7.7)	3.9 (1.6–11.1)	0.91	3.1 (1.5–8.5)	3.4 (1.9–7.7)	3.9 (1.6–11.1)	0.76
QUICKI	0.32 (0.29–0.40)	0.31 (0.27–0.34)	0.31 (0.29–0.35)	0.32	0.33 (0.28–0.37)	0.32 (0.30–0.35)	0.31 (0.29–0.34)	0.82
Muscle insulin resistance	2.1 (1.5–4.0)	1.7 (0.3–3.3)	3.0 (2.1–4.4)	0.20	2.0 (1.3–5.9)	2.4 (1.6–4.5)	1.9 (1.3–4.5)	0.80
Hepatic insulin resistance ($\times 10^6$)	5.3 (2.3–10.2)	5.0 (2.3–10.0)	3.7 (1.4–10.6)	0.66	3.9 (1.4–9.8)	4.3 (1.9–15.9)	4.5 (2.3–8.8)	0.75
Total cholesterol (mg/dl)	191 (128–276)	187 (129–252)	206 (163–244)	0.57	192 (114–224)	195 (136–273)	194 (162–234)	0.74
Triglycerides (mg/dl)	111 (28–224)	114 (36–204)	96 (36–521)	0.87	104 (22–241)	115 (57–241)	131 (36–173)	0.68
HDL cholesterol (mg/dl)	47 (35–82)	51 (31–73)	48 (20–74)	0.68	53 (40–71)	52 (39–64)	52 (36–79)	0.92
Platelets ($\times 10^4/\mu$l)	21.1 (9.4–30.8)	23.0 (7.0–38.2)	24.3 (20.2–41.2)	0.29	23.3 (14.5–27.6)	21.5 (6.3–31.8)	24.0 (15.2–32.6)	0.60
Ferritin (μg/dl)	185 (13–452)	397 (190–604)	46 (10–347)	0.14	74 (16–211)	162 (110–614)	62 (10–171)	0.05
hs-CRP	0.40 (0.08–7.53)	0.14 (0.02–0.61)	0.06 (0.00–0.30)	0.23	0.09 (0.04–0.23)	0.10 (0.00–0.24)	0.09 (0.00–0.89)	0.89
Type IV collagen 7S (ng/dl)	5.1 (2.7–10.0)	4.1 (3.1–7.2)	3.7 (3.3–4.5)	0.27	3.5 (2.3–3.9)	8.3 (3.2–14.0)	4.0 (3.2–5.0)	0.21
HA (ng/dl)	20.6 (0.0–144.7)	25.5 (11.5–299)	30.4 (0.0–61.7)	0.66	32.8 (0.0–117.2)	24.5 (0.0–570)	24.3 (0.0–140.3)	0.63
P-III-P (U/ml)	0.6 (0.5–1.2)	0.6 (0.4–45.0)	0.5 (0.4–0.6)	0.07	0.6 (0.3–0.8)	0.5 (0.5–233.0)	0.6 (0.4–1.0)	0.96
Diabetes (%)	82	69	64	0.59	82	75	64	0.56
Dyslipidemia (%)	73	63	73	0.95	73	63	73	0.86
Hypertension (%)	64	18	36	0.03	64	18	36	0.10
Metabolic syndrome (%)	73	38	27	0.18	67	50	45	0.43
ΔA1C					−1.9 (−6.0 to 0.4)	−1.2 (−6.1 to 4.4)	0.3 (−1.8 to 7.1)	0.02
ΔBody weight					−4.7 (−10.6 to 10.2)	2.2 (−9.4 to 13.4)	−0.9 (−12.7 to 9.6)	0.04
ΔHOMA-IR					−1.3 (−4.4 to 1.2)	−0.3 (−4.3 to 3.3)	−0.7 (−6.1 to 1.8)	0.81

Data are medians (range) or %. A Kruskal-Wallis test and a χ^2 test were used to compare the continuous and categorical variables among three groups. HA, hyaluronic acid; hs-CRP, high-sensitivity C-reactive protein; P-III-P, procollagen III peptide.

Liver fibrosis improved in 12 patients (30.7%), progressed in 11 patients (28.2%), and remained unchanged in 16 patients (41%). As shown in Table 1, fasting plasma glucose, A1C, insulin resistance indicators, and prevalence of metabolic disorders were not significantly different among the three liver fibrosis groups. In the Cox proportional hazard model (supplementary Table 3), although some of the confidence intervals were very wide because of the small sample size, improvement of liver fibrosis was significantly associated with changes in A1C between the initial and final liver biopsies (ΔA1C) ($P = 0.005$) and use of insulin for the treatment of diabetes ($P = 0.019$). Both ΔA1C and use of insulin were independently associated with the improvement of liver fibrosis after adjusted for each other. However, ΔA1C was more strongly associated with the improvement of liver fibrosis than use of insulin (χ^2; 7.97 vs. 4.58, respectively; supplementary Table 3).

CONCLUSIONS — In the present study, we showed that a change in glycemic control (ΔA1C), but not changes in insulin resistance indicators, was an independent predictor of the progression of liver fibrosis in Japanese patients with NAFLD. This is the first report identifying a change in A1C as a predictor of the histological course in the liver of patients with NAFLD. Two of five previous longitudinal studies have identified obesity, higher BMI, and homeostasis model assessment of insulin resistance (HOMA-IR) as predictors of liver fibrosis progression in Western populations (4,5). The difference between those results and the results of the present study may be due in part to differences in the assessed severity of obesity and insulin resistance between the populations. We previously demonstrated that diabetes is an independent risk factor for the progression of liver fibrosis in hepatitis C (6) and that diabetes accelerates the pathology of nonalcoholic steatohepatitis in the type 2 diabetic rat model OLETF (7).

Liver fibrosis is closely associated with two regulators of fibrosis: transforming growth factor (TGF)-β (8,9) and plasminogen activator inhibitor type 1 (PAI-1) (8,10). High glucose levels induce the expression of TGF-β (11) and PAI-1 (12). We previously reported that the expression of TGF family member genes, PAI-1, and genes involved in fibrogenesis are upregulated in the livers of patients with type 2 diabetes (13,14), suggesting that a diabetic state increases the risk for liver fibrosis.

In the present study, only ΔA1C was associated with the progression of liver fibrosis, but not liver inflammation (data not shown). We speculate that the reduction of A1C inhibits the expression of master genes such as *TGF-β* and *PAI-1* that are involved in the regulation of fibrogenesis, rather than genes involved in liver inflammation, and thereby improves liver fibrosis in NAFLD.

The major limitation of this study was small population size. We could not evaluate the changes of liver histology according to the difference in detail characteristics such as treatment of diabetes. Lower statistical power of this study should be consider when we evaluate the results.

In conclusion, our study suggested that ΔA1C could predict liver fibrosis progression in Japanese patients with NAFLD, and tight glycemic control may ameliorate liver fibrosis. Future large-scale prospective studies are needed to confirm our results.

Acknowledgments — This study was supported in part by a grant-in-aid from the Ministry of Education, Culture, Sports, Science and Technology, Japan.

No potential conflicts of interest relevant to this article were reported.

We thank Dr. Akiko Shimizu, Dr. Tsuguhito Ota, and Dr. Hirofumi Misu for recruiting the patients.

References

1. Duvnjak M, Lerotic I, Barsic N, Tomasic V, Virovic Jukic L, Velagic V. Pathogenesis and management issues for non-alcoholic fatty liver disease. World J Gastroenterol 2007;13:4539–4550
2. Sakurai M, Takamura T, Ota T, Ando H, Akahori H, Kaji K, Sasaki M, Nakanuma Y, Miura K, Kaneko S. Liver steatosis, but not fibrosis, is associated with insulin resistance in nonalcoholic fatty liver disease. J Gastroenterol 2007;42:312–317
3. Brunt EM, Janney CG, Di Bisceglie AM, Neuschwander-Tetri BA, Bacon BR. Nonalcoholic steatohepatitis: a proposal for grading and staging the histological lesions. Am J Gastroenterol 1999;94:2467–2474
4. Ekstedt M, Franzen LE, Mathiesen UL, Thorelius L, Holmqvist M, Bodemar G, Kechagias S. Long-term follow-up of patients with NAFLD and elevated liver enzymes. Hepatology 2006;44:865–873
5. Fassio E, Alvarez E, Dominguez N, Landeira G, Longo C. Natural history of nonalcoholic steatohepatitis: a longitudinal study of repeat liver biopsies. Hepatology 2004;40:820–826
6. Kita Y, Mizukoshi E, Takamura T, Sakurai M, Takata Y, Arai K, Yamashita T, Nakamoto Y, Kaneko S. Impact of diabetes mellitus on prognosis of patients infected with hepatitis C virus. Metabolism 2007;56:1682–1688
7. Ota T, Takamura T, Kurita S, Matsuzawa N, Kita Y, Uno M, Akahori H, Misu H, Sakurai M, Zen Y, Nakanuma Y, Kaneko S. Insulin resistance accelerates a dietary rat model of nonalcoholic steatohepatitis. Gastroenterology 2007;132:282–293
8. Matsuzawa N, Takamura T, Kurita S, Misu H, Ota T, Ando H, Yokoyama M, Honda M, Zen Y, Nakanuma Y, Miyamoto K, Kaneko S. Lipid-induced oxidative stress causes steatohepatitis in mice fed an atherogenic diet. Hepatology 2007;46:1392–1403
9. Uno M, Kurita S, Misu H, Ando H, Ota T, Matsuzawa-Nagata N, Kita Y, Nabemoto S, Akahori H, Zen Y, Nakanuma Y, Kaneko S, Takamura T. Tranilast, an antifibrogenic agent, ameliorates a dietary rat model of nonalcoholic steatohepatitis. Hepatology 2008;48:109–118
10. Bergheim I, Guo L, Davis MA, Lambert JC, Beier JI, Duveau I, Luyendyk JP, Roth RA, Arteel GE. Metformin prevents alcohol-induced liver injury in the mouse: critical role of plasminogen activator inhibitor-1. Gastroenterology 2006;130:2099–2112
11. Sugimoto R, Enjoji M, Kohjima M, Tsuruta S, Fukushima M, Iwao M, Sonta T, Kotoh K, Inoguchi T, Nakamuta M. High glucose stimulates hepatic stellate cells to proliferate and to produce collagen through free radical production and activation of mitogen-activated protein kinase. Liver Int 2005;25:1018–1026
12. Suzuki M, Akimoto K, Hattori Y. Glucose upregulates plasminogen activator inhibitor-1 gene expression in vascular smooth muscle cells. Life Sci 2002;72:59–66
13. Takamura T, Sakurai M, Ota T, Ando H, Honda M, Kaneko S. Genes for systemic vascular complications are differentially expressed in the livers of type 2 diabetic patients. Diabetologia 2004;47:638–647
14. Takeshita Y, Takamura T, Hamaguchi E, Shimizu A, Ota T, Sakurai M, Kaneko S. Tumor necrosis factor-alpha-induced production of plasminogen activator inhibitor 1 and its regulation by pioglitazone and cerivastatin in a nonmalignant human hepatocyte cell line. Metabolism 2006;55:1464–1472

CD14$^+$ Monocytes Are Vulnerable and Functionally Impaired Under Endoplasmic Reticulum Stress in Patients With Type 2 Diabetes

Takuya Komura,[1] Yoshio Sakai,[1] Masao Honda,[1] Toshinari Takamura,[1] Kouji Matsushima,[2] and Shuichi Kaneko[1]

OBJECTIVE—Although patients with diabetes suffer from increased infections and a higher incidence of cancer due to impaired immune function, details on diabetes-induced decrease in immunity are lacking. We assessed how immune-mediating peripheral blood mononuclear cells (PBMCs) are affected in diabetes.

RESEARCH DESIGN AND METHODS—From 33 patients with type 2 diabetes and 28 healthy volunteers, we obtained PBMCs and investigated their susceptibility to apoptosis and functional alteration.

RESULTS—In a subpopulation of PBMCs, monocytes derived from patients with diabetes were more susceptible to apoptosis than monocytes from healthy volunteers. Monocytes from patients with diabetes had decreased phagocytotic activity and were less responsive to Toll-like receptor (TLR) ligands, although the expression of TLRs did not differ significantly between the two groups. Furthermore, monocytes from patients with diabetes had a distinctly different gene expression profile compared with monocytes from normal volunteers as assessed with DNA microarray analysis. Specifically, quantitative real-time detection PCR measurements showed an elevated expression of the markers of endoplasmic reticulum (ER) stress in diabetic monocytes, and electron microscopic examination of monocytes revealed morphologic alterations in the ER of cells derived from patients with diabetes. Consistently, the ER stress inducer tunicamycin increased apoptosis of otherwise healthy monocytes and attenuated the proinflammatory responses to TLR ligands.

CONCLUSIONS—These data suggest that monocytes comprise a substantially impaired subpopulation of PBMCs in patients with diabetes and that ER stress is involved in these pathologic changes mechanistically. This implies that the affected monocytes should be investigated further to better understand diabetic immunity. ***Diabetes* 59:634–643, 2010**

Type 2 diabetes is the most frequent metabolic disease and the leading cause of human morbidity and mortality (1,2). Based on epidemiologic data, patients with diabetes are immunocompromised and have an increased incidence of infections in the respiratory tract, urinary tract, and skin (3–5). The high incidence of colorectal, breast, and pancreatic malignancies in patients with diabetes is also considered to be a consequence of diabetes-associated defects in immune function (6,7).

Although studies on immune cells and circulating cytokines have shed some light on this diabetic immunologic phenomenon, conflicting results have been reported and do not adequately explain the perturbed immune function in patients with diabetes. Controversial results concerning the phagocytotic activity of polymorphonuclear neutrophils and monocytes are in part due to differences in the patients themselves, insufficient numbers in the study populations, or inconsistencies in the collection of the cell populations under investigation (8–11). Therefore, further studies are needed to explain the decreased immune function of patients with diabetes.

We previously investigated the gene expression signatures of peripheral blood mononuclear cells (PBMCs) in patients with diabetes and observed transcriptional expression features that were distinct from those of healthy volunteers (12). Apoptosis-related genes were upregulated in the PBMCs of patients with diabetes. Based on this result, we investigated apoptotic activity and immunologic function in PBMCs from patients with type 2 diabetes.

We observed that the CD14$^+$ monocyte fraction was the most affected subpopulation of PBMCs from these patients; these cells were especially vulnerable to apoptosis compared with other cell subpopulations. We also found that CD14$^+$ monocytes demonstrated attenuated phagocytotic activity and deficient Toll-like receptor (TLR) signaling, both of which are important for innate immunity (13,14). Transcriptional analysis and electron microscopic examination of monocytes from patients with diabetes showed evidence of endoplasmic reticulum (ER) stress, which may underlie the functional defects in these cells. Collectively, the data presented herein show that CD14$^+$ monocytes are a vulnerable cell population under ER stress in these patients that could contribute to decreases in immune function in diabetes.

RESEARCH DESIGN AND METHODS

Thirty-three patients with type 2 diabetes (male/female, 15/18; age 62.0 ± 8.6 years; A1C 9.2 ± 2.0%) and 28 healthy volunteers (male/female, 15/13; age 58.2 ± 10.2 years; A1C 5.4 ± 0.7%) were enrolled consecutively for the

From [1]Disease Control and Homeostasis, Kanazawa University, Graduate School of Medical Science, Kanazawa, Japan; and the [2]Department of Molecular Preventive Medicine, School of Medicine, The University of Tokyo, Tokyo, Japan.

Corresponding author: Shuichi Kaneko, skaneko@m-kanazawa.jp.

Received 13 May 2009 and accepted 16 November 2009. Published ahead of print at http://diabetes.diabetesjournals.org on 3 December 2009. DOI: 10.2337/db09-0659.

TABLE 1
Characteristics of the study subjects

	Diabetic patients (n = 33)	Healthy volunteers (n = 28)	P
Age (years)	62.0 ± 8.6	58.2 ± 10.2	NS
Sex (male/female)	15/18	15/13	NS
BMI (kg/m^2)	23.5 ± 4.2	23.6 ± 4.8	NS
White blood cell counts (ml)	4,800 ± 1,700	5,600 ± 1,900	NS
Lymphocytes (%)	23.5 ± 3.5	22.7 ± 2.5	NS
Monocytes (%)	5.2 ± 1.6	6.1 ± 2.3	NS
Hemoglobin (g/dl)	14.1 ± 1.3	13.6 ± 1.6	NS
Total cholesterol (mg/dl)	182 ± 24	180 ± 35	NS
Triglyceride (mg/dl)	138 ± 37	163 ± 33	NS
FPG (mg/dl)	185 ± 38	86 ± 7.4	<0.001
A1C (%)	9.2 ± 2.0	5.4 ± 0.7	<0.001
Diabetic complications (+/−)*	19/14	NA	
Insulin treatment (+/−)	10/23	NA	

Data are means ± SD. *Diabetic complications: nephropathy, neuropathy, retinopathy, macroangiopathy. FPG, fasting plasma glucose; NA, not applicable.

apoptosis assay (Table 1). The groups were not significantly different in terms of their clinical parameters, except for the fasting plasma glucose and A1C levels. The patients with diabetes (n = 16) from whom adequate numbers of monocytes were obtained were enrolled for additional experiments along with 17 other patients with diabetes (male/female, 8/9; age 60.5 ± 7.2 years; A1C 8.8 ± 1.8%) whose clinical profiles fit the diabetic profile (Table 1). Informed consent for this study was obtained from all subjects. The experimental protocol was carried out in accordance with the Declaration of Helsinki.

Isolation of subpopulations of PBMCs and flow cytometric analysis. PBMCs were freshly isolated from heparinized venous blood using Ficoll-Hypaque (Sigma-Aldrich, St. Louis, MO) as previously described (12). CD4$^+$ T-cell and CD14$^+$ monocyte subpopulations were isolated using a magnetic cell sorting system in accordance with the manufacturer's protocol (Miltenyi Biotec, Bergisch Gladbach, Germany). Isolated cells were purified by >90% as measured by flow cytometric analysis using FACSCalibur flow cytometer (BD Biosciences, San Jose, CA). To assess the expression of TLRs on monocytes, PBMCs were incubated with phosphatidylethanolamine (PE)-labeled anti-TLR2, -TLR3, or -TLR4 (eBioscience, San Diego, CA) and fluorescein isothiocyanate (FITC)-labeled anti-CD14 antibodies (BD Biosciences) and analyzed by flow cytometry. Data were analyzed using CELLQuest Software (BD Biosciences).

Quantitative real-time detection PCR. Real-time detection (RTD)-PCR was performed as previously described (15). Briefly, total RNA obtained from cells using a MicroRNA isolation kit (Stratagene, La Jolla, CA) was reverse-transcribed using 1 μg oligo (dT) primer and Super Script II Reverse transcriptase (Invitrogen, Carlsbad, CA). The relative quantities of mRNA expression were analyzed by RTD-PCR using ABI PRISM 7900 HT Sequence Detection System (Applied Biosystems, Foster City, CA). All primer pairs and probes were obtained from the TaqMan assay reagents library. Expression levels of genes were calculated with the $2^{-\Delta\Delta Ct}$ method using either β-actin or GAPDH as internal control genes.

Apoptotic cell detection assay. Freshly isolated PBMCs were incubated with AIM-V (Invitrogen) serum-free culture media containing 5 or 30 mmol/l glucose at 37°C with 5% CO_2 for up to 24 h. The cells were incubated with FITC-labeled anti-CD4, -CD14, or -CD56 antibodies (BD Biosciences) and with PE-labeled annexin-V and 7-amino-actinomycin D (7-AAD) (BD Biosciences) in PBS containing 2% BSA (Sigma-Aldrich). Apoptotic cells were determined by flow cytometry as the fraction of cells labeled with annexin-V that were 7-AAD negative. At least 10,000 cells per sample were analyzed.

Phagocytosis assay. Phagocytotic activity was assessed using a Phagotest Kit (Orpegen Pharma, Heidelberg, Germany) and FITC-labeled opsonized *Escherichia coli* in accordance with the manufacturer's protocol. Briefly, heparinized whole blood obtained from the 33 patients with diabetes and 28 healthy volunteers was incubated with FITC-labeled *E. coli* for 10 min at 37°C. After removing the erythrocytes, the remaining cells were incubated with propidium iodide to detect viable leukocytes by flow cytometry. Monocyte populations were assessed based on cellular granularity and size as side scatter and forward scatter, respectively, and FITC-positive cells were assessed as monocytes with phagocytosed FITC-labeled *E. coli*.

TLR ligand stimuli and expression of proinflammatory cytokine genes. Peptidoglycan (PGN; 1 μg/ml) from *Streptomyces sp.* (Sigma-Aldrich), Poly (I:C) (5 μg/ml; Sigma-Aldrich), and lipopolysaccharide (LPS; 2 μg/ml) from *E. coli* (Sigma-Aldrich), which are TLR2, TLR3, and TLR4 ligands, respectively, were added to monocytes (3×10^5 cells) freshly isolated from the 33 patients and 28 healthy volunteers in AIM-V media. Before and 3 h after incubation, the expression of tumor necrosis factor-α (TNF-α) and interleukin-1β (IL-1β) was analyzed by RTD-PCR.

Analysis of gene expression by DNA microarray. Total RNA was obtained from CD14$^+$ monocytes using MicroRNA isolation kit (Stratagene), and the mRNA was amplified twice using the Amino Allyl MessageAmp aRNA Kit (Ambion, Austin, TX). The reference RNA sample was isolated from CD14$^+$ monocytes from a 30-year-old healthy male volunteer and amplified in the same manner. Amplified mRNA was labeled with cyanin (Cy) 5 or Cy3 (Amersham, Buckinghamshire, U.K.). Equal amounts of the amplified mRNAs were hybridized to an oligo-DNA chip (AceGene Human Oligo Chip 30K; Hitachi Software Engineering, Yokohama, Japan) overnight and washed prior to image scanning.

The fluorescence intensity of each spot on the oligo-DNA chip was obtained using cDNA Microarray Scan Array G (PerkinElmer, Wellesley, MA). The obtained images were quantified using DNAsis array V2.6 software (Hitachi Software Engineering). For normalization, the intensity of each spot with oligo DNA was subtracted from that of spots without oligo DNA in the same block. The spot was validated when the intensity was within the intensity plus or minus a twofold range of SD within each block. By calibrating the median as the base value, the intensities of all spots were adjusted for normalization between Cy5 and Cy3. Hierarchic clustering of gene expression was calibrated using the method described above using BRB Array Tools (http://linus.nci.nih.gov/BRB-ArrayTools.html). The nonfiltered data were log-transformed and applied to the average linkage clustering with centered correlation. For the functional analysis of the 813 upregulated genes, we used GenMAPP (http://www.genmapp.org), a computer program designed for viewing and analyzing genome-scale data on MAPPs representing biological pathways and any other groups of genes.

Electron microscopy. Monocytes obtained from three healthy volunteers and three patients with diabetes were fixed with 2.5% glutaraldehyde and then postfixed in 1% (vol/vol) cacodylate-buffered osmium tetroxide. Samples were dehydrated in a graded series of ethanol, transferred to propylene oxide, and embedded in Epon-Araldite (Sigma-Aldrich). Ultrathin sections were obtained and observed under a Hitachi H-7500 electron microscope (Hitachi High-Technologies, Hitachinaka, Japan).

Caspase-3 assay and enzyme-linked immunosorbent assay (ELISA) of cytokines. Monocytes from a healthy volunteer were harvested and treated with tunicamycin (1 or 5 μg/ml) in AIM-V media. Every 3 h up to 12 h after tunicamycin treatment, we assessed apoptosis by flow cytometry as described above. After 12 h of incubation, the expression levels of BCL-2, C/EBP homologous protein (CHOP), and BiP (immunoglobulin heavy chain binding protein) were assessed by RTD-PCR. The DEVD-cleaving activity of active caspase-3 was measured using labeled Asp-Glu-Val-Asp-p-nitroanilide (DEVD-pNA) as the substrate and the Caspase-3 Colorimetric Assay Kit (Promega, Madison, WI) in accordance the manufacturer's protocol. The pNA light emission was quantified using a microtiter plate reader at a wavelength of 405 nm. In addition, we measured the production of proinflammatory cytokines by RTD-PCR 6 h after treatment of monocytes (3×10^5 cells) with tunicamycin (1 or 5 μg/ml) or the TLR ligands PGN (1 μg/ml), Poly (I:C) (5 μg/ml), and LPS (2 μg/ml). The concentrations of TNF-α, IL-1β, and IL-6 in the culture supernatants were measured using an ELISA kit (eBioscience).

Statistical analysis. Data are expressed as means ± SEM. The Mann-Whitney U test was applied to assess the significant differences between the two groups. Statistical significance was determined as $P < 0.05$, $P < 0.01$, and $P < 0.001$.

RESULTS

Increased apoptosis of CD14$^+$ monocytes from patients with diabetes. We first assessed the frequency of apoptosis in the PBMC fractions from 33 patients with diabetes and 28 nondiabetic healthy volunteers. Apoptosis of the isolated cells was assessed after 3-h incubation in AIM-V serum-free media containing 5 mmol/l glucose (physiological concentration in blood). As shown in Fig. 1*A*, a significant difference in the frequency of apoptosis was observed in the PBMCs isolated from patients with diabetes and healthy volunteers. Adding serum to AIM-V serum-free media did not affect the difference in apoptosis (data

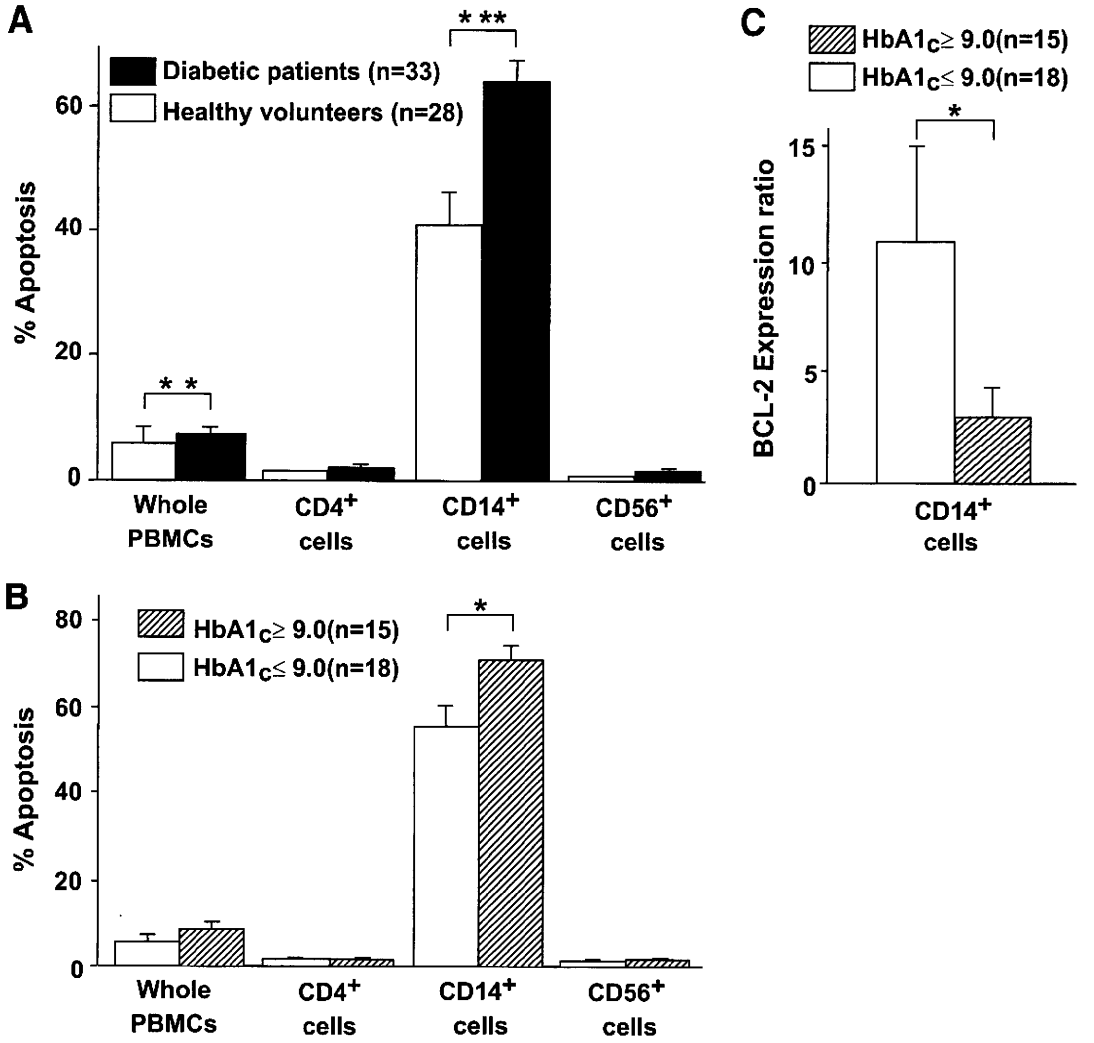

FIG. 1. Monocytes contributed to the vulnerability of the PBMCs in patients with diabetes. *A*: PBMCs were obtained from 33 patients with diabetes and 28 healthy volunteers. Isolated PBMCs were harvested in AIM-V serum-free culture media supplemented with 5 mmol/l glucose for 3 h and incubated with FITC-labeled anti-CD4, -CD14, or -CD56 antibodies, together with PE-labeled annexin-V to assess the frequency of apoptotic cells in each subpopulation of PBMCs. Apoptotic cells were identified by double-staining with PE-labeled annexin-V and 7-AAD by flow cytometry. The frequencies of apoptotic cells determined as the annexin-V–positive and 7-AAD–negative population are expressed as means ± SEM with statistical comparisons for both groups. The nonparametric Mann-Whitney *U* test was used to calculate the *P* value. $^{**}P < 0.01$, $^{***}P < 0.001$. The PBMCs of patients with diabetes were more susceptible to apoptosis than those of healthy volunteers, and $CD14^+$ monocytes were contributors. *B*: Among the 33 patients with diabetes, those with poor glycemic control reflected as A1C ≥9.0% were more susceptible to apoptosis in $CD14^+$ monocytes. Data are expressed as means ± SEM with a statistical comparison of both groups. $^*P < 0.05$. *C*: Monocytes were isolated from 15 patients with A1C ≥9.0% and 18 patients with A1C <9.0%. The expression of the BCL-2 gene in their monocytes before and after incubation in AIM-V serum-free media was assessed by RTD-PCR. After 3-h incubation, the expression of BCL-2 was not upregulated in the poor glycemic control group (A1C ≥9.0%), compared with the fair control group (A1C <9.0%). Data are expressed as means ± SEM with statistical comparisons of both groups. $^*P < 0.05$.

not shown). The numbers of whole PBMCs and $CD4^+$, $CD14^+$, and $CD56^+$ cells were similar in both diabetic and healthy subjects (data not shown). $CD14^+$ monocytes were observed to be the major contributor to the increased apoptosis measured in the PBMCs. In contrast, apoptosis of $CD4^+$ T-cells and $CD56^+$ natural killer (NK) cells was not significantly different between the two groups (Fig. 1*A*). When the incubation period in culture media with or without serum was extended to 24 h, ~20% of the $CD56^+$ NK cells of both patients with diabetes and healthy volunteers were induced to undergo apoptosis. When incubation period was extended to 5 days, ~5% of $CD4^+$ T-cells of both patients with diabetes and healthy volunteers were induced to undergo apoptosis; there was no significant difference in cell viability of $CD56^+$ NK cells and $CD4^+$ T-cells between the two groups (data not shown). BCL-2 expression of $CD4^+$ T-cells was not different between the two groups (data not shown). Apoptosis of PBMC subpopulations incubated in culture media containing 30 mmol/l glucose was not different from cells incubated in 5 mmol/l glucose-containing media (data not shown). Moreover, the susceptibility of PBMCs from patients with diabetes to apoptosis was not related to clinical features such as vascular complications, insulin treatment, and fasting plasma glucose concentrations (data not shown).

However, among the 33 patients with diabetes, the frequency of apoptotic $CD14^+$ monocytes from those with poor glycemic control (A1C ≥9.0%) was elevated compared with patients with fair glycemic control (A1C <9.0%) (Fig. 1*B*). Furthermore, after 3-h incubation, the increased ratio of the expression of the antiapoptotic gene, BCL-2, was substantially lower in monocytes from the 15 patients with A1C ≥9.0% compared with the 18

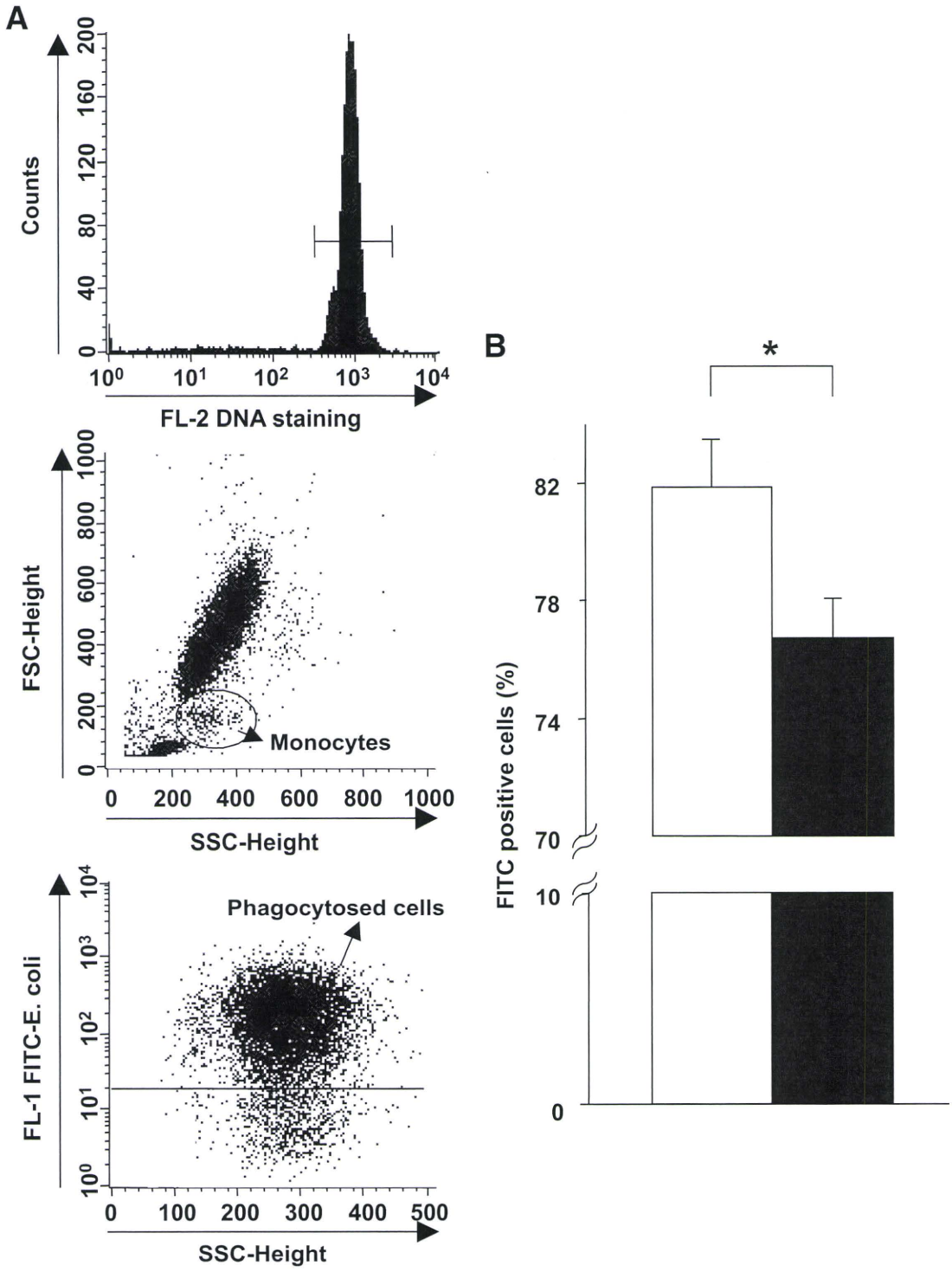

FIG. 2. Attenuated phagocytosis activity in diabetic monocytes. Whole PBMCs were incubated with FITC-labeled *E. coli* for 10 min followed by propidium iodide staining and flow cytometric analysis. *A*: Gated propidium iodide–positive populations were viable leukocyte populations (*upper panel*). The monocyte population was assessed using granularity (side scatter) and size (forward scatter) (*middle panel*). For the gated cells indicating viable monocytes, FITC-positive cells were assessed as monocytes containing phagocytosed FITC-labeled *E. coli* (*lower panel*). *B*: The frequency of monocytes containing phagocytosed *E. coli* in patients with diabetes (■, $n = 33$) was less than that in healthy volunteers (□, $n = 28$). Data are expressed as means ± SEM. *$P < 0.05$.

patients having A1C <9.0%, as assessed by RTD-PCR (Fig. 1*C*). These data suggest that the monocytes of patients with diabetes are susceptible to apoptosis, especially under conditions of poor glycemic control.

Attenuated function of monocytes from patients with diabetes. To determine whether functional alterations exist in monocytes isolated from the 33 patients with diabetes, we cocultured the monocytes with FITC-labeled *E. coli* and counted the number of fluorescent monocytes that phagocytosed the labeled *E. coli* by flow cytometry. The ratio of monocytes that phagocytosed *E. coli* to all monocytes in patients with diabetes was higher than in the healthy volunteers (Fig. 2*A* and *B*). No significant correlation was observed between the ratio of phagocy-

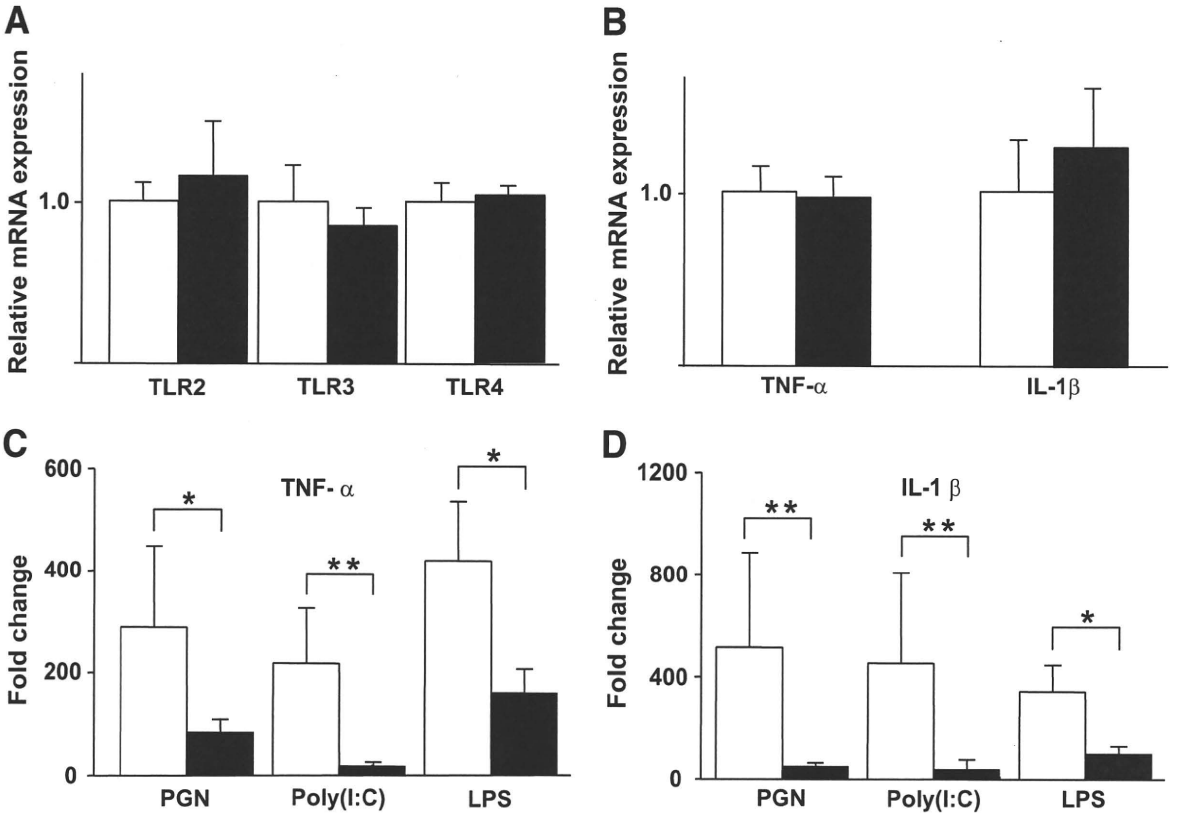

FIG. 3. Hyporesponsiveness to TLR ligand stimuli by the monocytes of patients with diabetes. *A–D*: Isolated CD14$^+$ monocytes from 33 patients with diabetes (■) and 28 healthy volunteers (□) were cultured in AIM-V serum-free media supplemented with each TLR ligand: PGN, Poly (I:C), and LPS. After 3-h incubation, RNA was isolated from the monocytes, and the expression levels of the TNF-α and IL-1β genes were analyzed by RTD-PCR. The basal (prestimuli) expression of TLR2, TLR3, and TLR4 (*A*) and TNF-α and IL-1β (*B*) did not differ significantly between the two groups. The TLR ligand–induced expression of TNF-α (*C*) and IL-1β (*D*) was downregulated in the monocytes of patients with diabetes. Data are expressed as means ± SEM. *$P < 0.05$, **$P < 0.01$.

tosed *E. coli* and A1C levels among the patients (data not shown).

Next, we assessed the responsiveness of monocytes to external pathogenic stimuli in vitro. Monocytes typically express pattern-recognition molecules such as the TLRs that are important for innate immunity against various pathogens (13,14). The expression levels of TLR2, TLR3, and TLR4 were not significantly different between monocytes from patients with diabetes and those from healthy volunteers, as assessed by RTD-PCR (Fig. 3*A*) and flow cytometry (data not shown). We also found that transcriptional expression of TLR signal molecules (MyD88, IRAK1, and TRAF6 for TLR2 and TLR4 signaling and TRIF for TLR3 signaling) was not altered in diabetic monocytes compared with nondiabetic monocytes (data not shown). Next, we exposed the monocytes from the patients with diabetes and healthy volunteers to the TLR ligands, PGN (a TLR2 ligand), Poly (I:C) (a TLR3 ligand), and LPS (a TLR4 ligand) and measured the expression of the proinflammatory cytokine genes, TNF-α and IL-1β. After incubation, the expression of the cytokines was not significantly different between the groups (Fig. 3*B*), but the responsiveness to PGN, Poly (I:C), and LPS was significantly attenuated in monocytes from patients with diabetes compared with those from healthy volunteers as assessed by RTD-PCR (Fig. 3*C* and *D*). These results demonstrate that the monocytes of patients with diabetes are functionally impaired, which implies that they could contribute to immune deficiency in diabetes.

ER stress is a molecular feature of impaired monocytes. To elucidate the molecular features of the diabetic monocytes that were distinctly susceptible to apoptosis, DNA microarray analysis was performed on CD14$^+$ cells isolated from five randomly selected patients with diabetes and five healthy volunteers. These subjects demonstrated clinical features near the median of all study subjects. Unsupervised hierarchic clustering analysis was performed to assess the gene expression profiles of monocytes obtained from patients with diabetes and healthy volunteers; 17,184 filtered genes were evaluated after excluding genes that were not expressed or those with low expression levels that prevented their analysis in 50% of the cases. As shown in Fig. 4*A*, two completely discernible clusters formed between the patients with diabetes and the healthy volunteers.

We identified 813 genes that were upregulated in the monocytes from patients with diabetes compared with those of healthy volunteers ($P < 0.05$, Student t test). Analysis of the biological processes concerning these genes was performed using GenMAPP. The identified genes were shown to be involved in posttranslational protein modification systems occurring in the Golgi apparatus or were involved in ER stress (Table 2 and supplementary Table 1, available in an online appendix at http://diabetes.diabetesjournals.org/cgi/content/full/db09-0659/DC1). The elevated expression of genes related to ER stress, such as CHOP and BiP, was confirmed using RTD-PCR; the expression of these genes was significantly higher in the monocytes from the 33

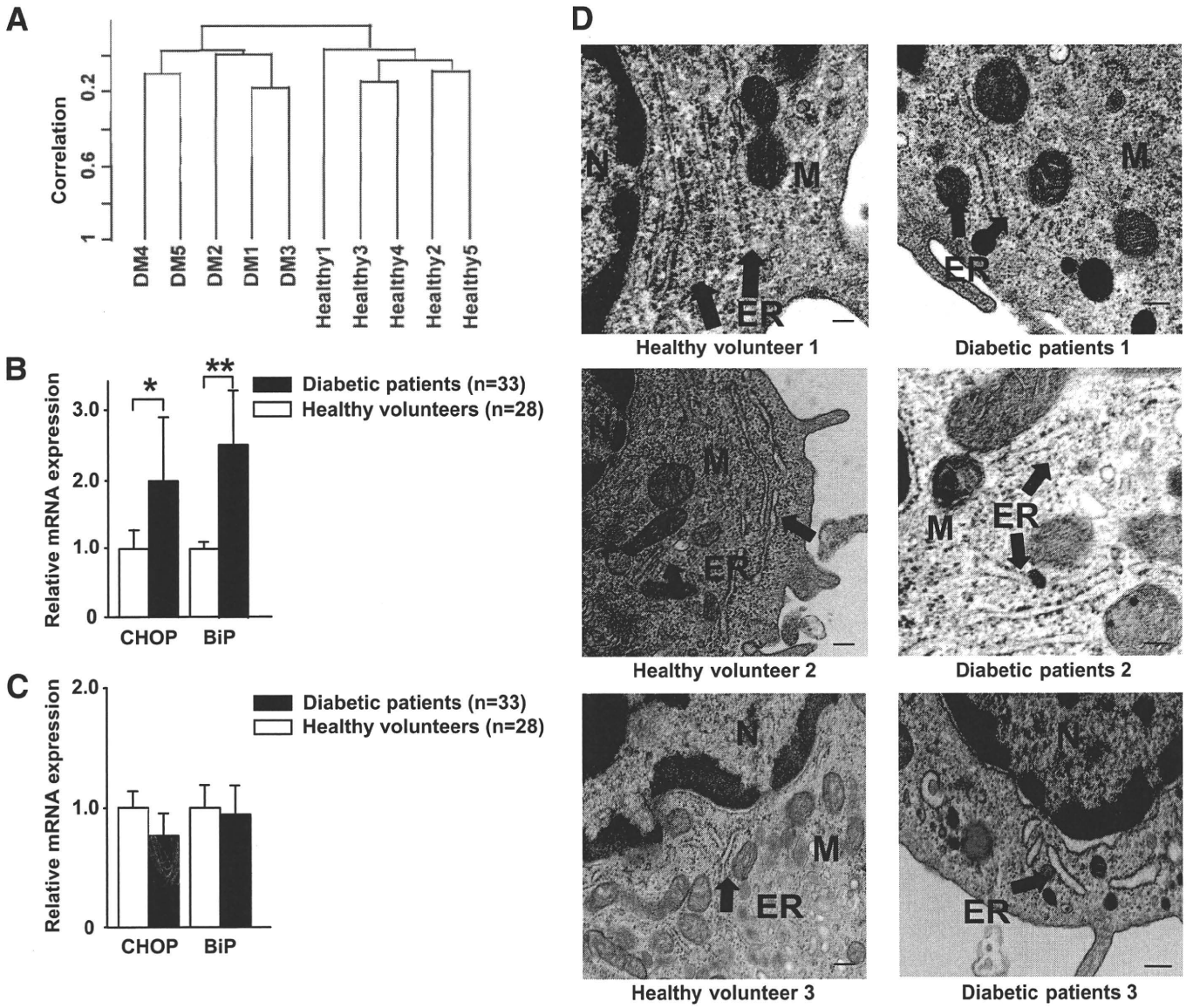

FIG. 4. Monocytes of patients with diabetes were under ER stress. *A*: The gene expression profiles of representative vulnerable CD14$^+$ monocytes obtained from five patients with diabetes and five healthy volunteers were analyzed using a DNA microarray. Unsupervised hierarchic clustering using 17,184 filtered genes produced two clusters that separated the patients with diabetes from the healthy volunteers without exception. *B* and *C*: The gene expression levels of the ER stress markers, such as CHOP and BiP, on CD14$^+$ monocytes and CD4$^+$ T-cells obtained from 33 patients with diabetes and 28 healthy volunteers were analyzed using RTD-PCR. *B*: The expression levels of CHOP and BiP in monocytes of patients with diabetes were significantly upregulated, compared with the monocytes of healthy volunteers. Data are expressed as means ± SEM. *$P < 0.05$, **$P < 0.01$. *C*: The expression levels of CHOP and BiP in T-cells of patients with diabetes were similar to those of healthy volunteers. Data are expressed as means ± SEM. *D*: Monocytes were obtained from three healthy volunteers and three patients with diabetes (healthy volunteer 1: 64-year-old man, A1C 5.7%; healthy volunteer 2: 66-year-old man, A1C 4.9%; healthy volunteer 3: 68-year-old woman, A1C 5.6%; diabetic patient 1: 56-year-old man, A1C 9.1%; diabetic patient 2: 64-year-old woman, A1C 8.2%; diabetic patient 3: 71-year-old man, A1C 10.2%) and examined using electron microscopy. In the three patients with diabetes, the concentric, continuous, and regular layer structures of the ER were corrupted, with fewer ribosomes on the ER membrane compared with the ER of the healthy volunteer. ER, endoplasmic reticulum; M, mitochondrion; N, nucleus. Scale bars indicate 100 nm.

patients with diabetes than in those from the 28 healthy volunteers (Fig. 4*B*). In contrast, no significant difference in the expression of these genes was observed in CD4$^+$ T-cells from patients with diabetes and healthy volunteers (Fig. 4*C*).

Electron microscopy further confirmed ER stress in the monocytes derived from patients with diabetes. As shown in Fig. 4*D*, morphologic alterations of the ER such as corruption of concentric, continuous, and regular layer structure and a decreased number of ribosomes on the ER membrane were evident from the electron photomicrographic images.

ER stress–induced apoptosis and attenuation of TLR signaling in human monocytes. The results described above indicated that the monocytes from patients with diabetes have compromised immunologic function and that ER stress is a distinct feature in these cells. To determine whether ER stress could be a mechanism underlying the observed increase in apoptosis and decreased responsiveness to TLR ligands, CD14$^+$ cells isolated from a healthy volunteer were treated with the ER stress inducer, tunicamycin (1 μg/ml), in AIM-V media. As shown in Fig. 5*A* and *B*, an increased number of apoptotic cells was observed among monocytes treated with tunica-

TABLE 2
Biological processes for upregulated genes in monocytes of diabetic patients

	Z score	Permute *P* value
MAPP name		
Golgi apparatus	3.383	0.000
Ribosomal proteins	3.691	0.002
Unfold protein binding	2.471	0.026
Intracellular protein transport	2.310	0.029
Enzyme-linked receptor protein signaling pathway	2.175	0.042
Nuclear receptor	2.316	0.043
Gametogenesis	−1.998	0.049

mycin compared with untreated monocytes after >6 h of incubation. Treatment of monocytes with a higher concentration of tunicamycin (5 μg/ml) induced more apoptosis (Fig. 5*A* and *B*), and when monocytes were treated with tunicamycin for 12 h, the activity of the proapoptotic protease, caspase-3, significantly increased (Fig. 5*C*). Treatment with tunicamycin coordinately decreased the expression of BCL-2 (Fig. 5*D*) and increased the expression of the ER stress markers, CHOP and BiP (Fig. 5*E*). These results suggest that ER stress promotes apoptosis of human monocytes.

Next, we investigated how tunicamycin-induced ER stress affected the responsiveness of human monocytes to TLR ligands. Treatment of monocytes with tunicamycin for 6 h did not affect the transcriptional and translational expression of TLR2 and TLR4 (data not shown). As shown in Fig. 6*A–C*, however, the expression of the proinflammatory cytokines TNF-α, IL-1β, and IL-6 was downregulated after stimulation with TLR2 and TLR4 ligands. Furthermore, the production of TNF-α, IL-1β, and IL-6 in media was measured by ELISA and found to decrease after treatment of human monocytes with tunicamycin and after stimulation with TLR2 or TLR4 ligands (Fig. 6*D–F*). However, tunicamycin-induced ER stress did not affect expression after treatment of monocytes with the TLR3 ligand, Poly (I:C) (data not shown).

DISCUSSION

In the present study, we observed that PBMCs from patients with diabetes were more susceptible to apoptosis compared with PBMCs from healthy volunteers and that

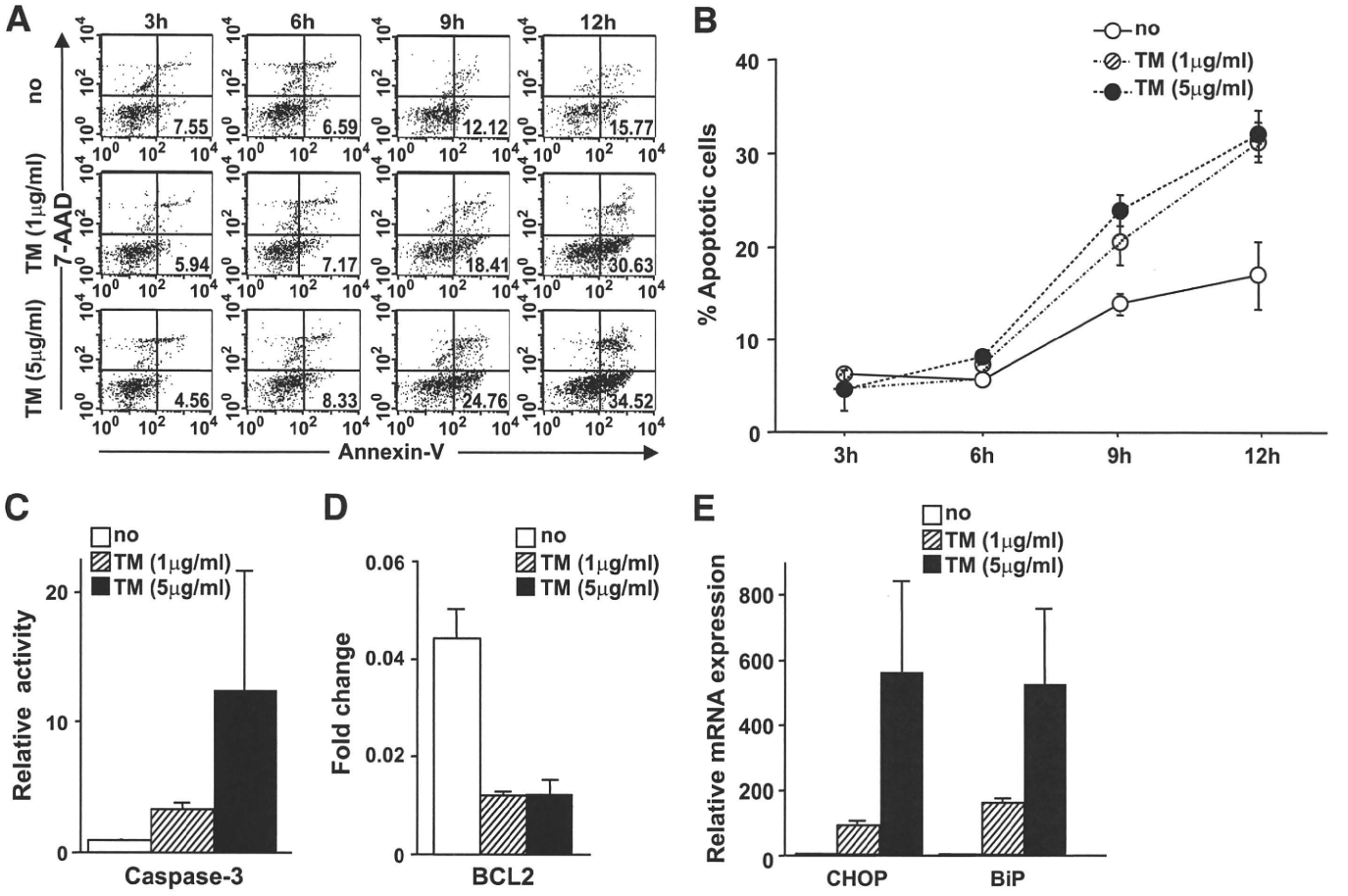

FIG. 5. ER stress enhanced the susceptibility of human monocytes to apoptosis. *A* and *B*: Human CD14$^+$ monocytes obtained from a healthy volunteer were incubated in AIM-V culture media supplemented with tunicamycin (TM) (1 or 5 μg/ml). The frequency of apoptotic cells was analyzed by flow cytometry every 3 h for 12 h. More apoptotic cells were observed among monocytes treated with tunicamycin for >6 h of incubation, compared with untreated monocytes. *A*: Representative scattergram of annexin-V and 7-AAD for monocytes treated with tunicamycin. The numbers in each quadrant indicate the percentage of apoptotic cells. *B*: Apoptotic cells were assessed in triplicate for each condition. Data are expressed as means ± SEM. *C*: Caspase-3 activity in monocytes treated with tunicamycin increased significantly at 12 h of incubation. *D*: The BCL-2 expression in monocytes incubated with tunicamycin for 12 h was downregulated. *E*: The expression levels of the ER stress markers CHOP and BiP in monocytes incubated with tunicamycin for 12 h were significantly upregulated. Data are expressed as means ± SEM of three independent experiments. □, No treatment; ▨, treatment with tunicamycin (1 μg/ml); ■, treatment with tunicamycin (5 μg/ml).

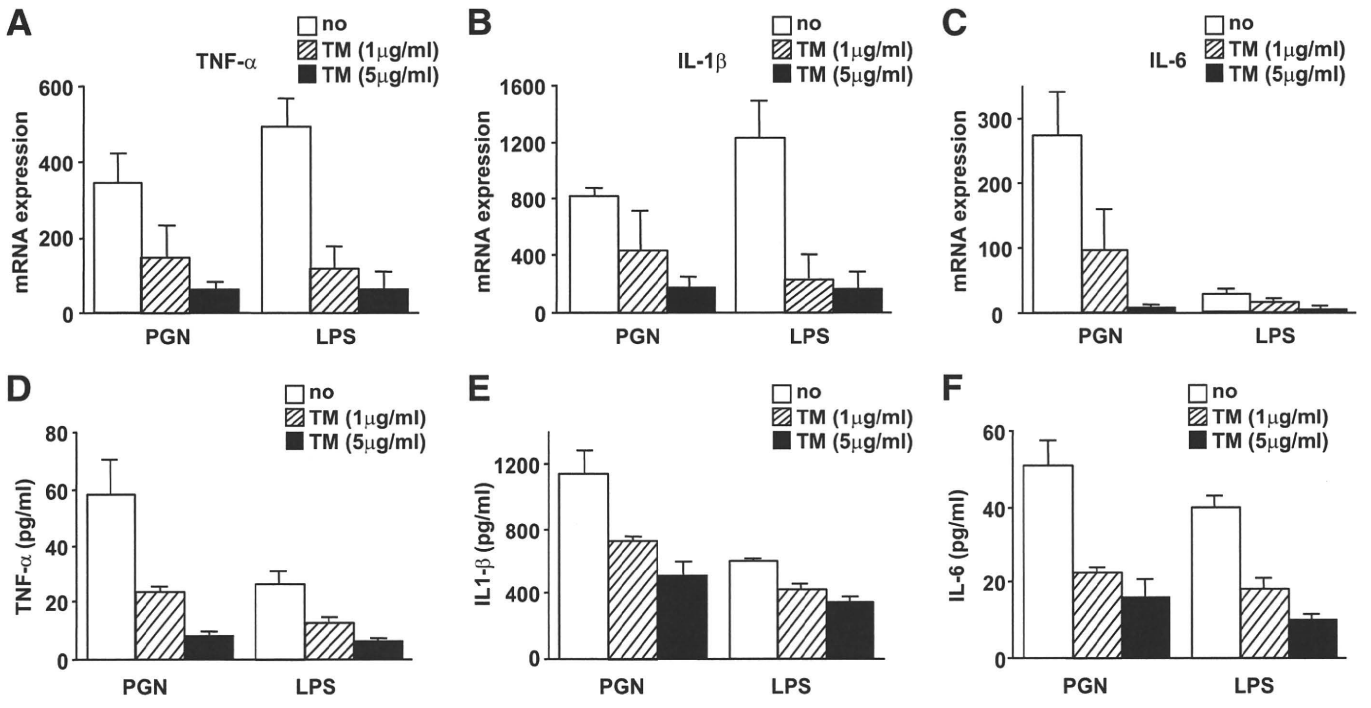

FIG. 6. Expression of proinflammatory cytokines in response to TLR ligand stimuli decreased in human monocytes treated with tunicamycin (TM). Isolated human CD14$^+$ monocytes were incubated in AIM-V culture media with tunicamycin (1 or 5 μg/ml) and stimulated using TLR ligands, PGN, and LPS for 6 h. *A–C*: RTD-PCR analysis showed that the expression of TNF-α (*A*), IL-1β (*B*), and IL-6 (*C*) was downregulated in human CD14$^+$ monocytes treated with tunicamycin, especially at the higher concentration (5 μg/ml). *D–F*: ELISA showed that the production of TNF-α (*D*), IL-1β (*E*), and IL-6 (*F*) in culture media decreased in human monocytes treated with tunicamycin, especially at the higher concentration (5 μg/ml). Data are expressed as means ± SEM of four independent experiments. □, No treatment; ▨, treatment with tunicamycin (1 μg/ml); ■, treatment with tunicamycin (5 μg/ml).

CD14$^+$ monocytes comprised the primary PBMC subpopulation undergoing apoptosis. We also found that CD14$^+$ monocytes from patients with diabetes were hyporesponsive to TLR ligands and that they had attenuated phagocytotic activity. Transcriptional analysis and electron microscopy revealed the presence of ER stress in the affected diabetic monocytes. Consistently, monocytes isolated from nondiabetic patients showed a similar increase in apoptosis and a weakened response to TLR ligands, when they were treated with tunicamycin, indicating that ER stress may be a pivotal mechanism underlying the decreased immunologic function observed in patients with diabetes.

As innate immune-defense mediators, monocytes are capable of ingesting exogenous pathogens to protect the host from infectious diseases. Previous studies have shown that phagocytosis in diabetic neutrophils and monocytes is attenuated (10,11). Similarly, in our study population, monocytes from patients with diabetes were less capable of phagocytosing *E. coli* pathogens compared with monocytes derived from healthy volunteers. This novel finding might explain, at least in part, the decrease in immune function characteristic of patients with diabetes (16). Nevertheless, the detailed mechanisms underlying diabetes-induced decreases in phagocytotic activity remain unclear, because simple high-glucose concentration neither affected the phagocytotic activity and TLR expression nor induced ER stress in nondiabetic monocytes in vitro (data not shown).

The TLRs are pattern-recognition receptors that are important for recognizing pathogens, inducing proinflammatory responses, and preventing the host from acquiring infectious diseases (17–20). The expression of TLR2, TLR3, and TLR4 in CD14$^+$ monocytes was similar between patients with diabetes and healthy volunteers. The administration of a high dose of insulin downregulates TLR expression (21). Transformed monocyte-lineage blastoma cells showed increased TLR expression under hyperglycemic conditions in vitro (22). Type 2 diabetes is characterized as a state of inadequately controlled glycemia associated with hyperinsulinemia due to peripheral insulin resistance (1). Taken together, the TLR expression may be affected by hyperglycemia and hyperinsulinemia in a complex manner. In contrast to the previous finding that monocytes from patients with diabetes were hypersensitive to the TLR ligand, LPS (23,24), we observed that the TNF-α and IL-1β expression from monocytes derived from patients with type 2 diabetes diminished after exposure to PGN, Poly I:C, and LPS—ligands of the TLR2, TLR3, and TLR4 receptors, respectively. These data suggest that diabetes perturbs signaling downstream of the TLRs. In this study, we collected CD14$^+$ monocytes from PBMCs via enrichment using magnetic beads; this protocol was used to remove T-cells, NK cells, B-cells, dendritic cells, and basophils from the PBMC mixture. This is in contrast to the methodology used to isolate these cells in many other studies, in which monocytes were obtained as adherent cells in the culture dish or by a rosetting technique (25,26). CD14$^+$ cells have been shown to be composed of multiple subtypes of activated states; the classical monocyte-isolation methods used in the other studies might unknowingly remove the fraction of monocytes that are susceptible to apoptosis (27). More than half of the CD14$^+$ diabetic monocytes isolated in this study were dead after 12-h incubation, even in media containing physiological concentration of glucose (data not shown).

Our current data showing attenuation of TLR responsiveness to ligands in diabetic monocytes suggest that initial immune responses that are normally triggered by viruses, bacteria, and parasites could be impaired in diabetes, which is consistent with epidemiologic data showing a high incidence of infection in patients with diabetes (3–5).

Gene expression and electron microscopic analysis of monocytes derived from patients with diabetes showed active signatures of ER stress; this is important because ER is an organelle essential for the proper folding and glycosylation of proteins after protein synthesis (28). When cells are under ER stress, protein kinase R–like ER kinase, inositol-requiring enzyme 1, and activating transcription factor 6 are activated and function in the adaptation to stress, proper folding of proteins, and removal of harmful unfolded proteins, respectively (29,30). However, prolonged ER stress leads to apoptotic cell death, which is mediated by CHOP (31). CHOP is a crucial and specific molecule for ER stress–induced apoptosis and alters the transcription of the *BCL-2* gene family members (32). The current study showed that diabetic monocytes had increased levels of ER stress–related apoptotic molecules. Moreover, nondiabetic monocytes treated with tunicamycin, an ER stress inducer, underwent apoptosis in a manner similar to monocytes derived from patients with diabetes. From these data, we conclude that ER stress contributes to the susceptibility of diabetic monocytes to apoptosis.

We also observed that tunicamycin-induced ER stress diminished TLR2 and TLR4 signaling without altering expression of TLRs. Tunicamycin induces ER stress by disturbing N-linked glycosylation (33), and previous reports suggest that perturbations in this glycosylation attenuate TLR2 and TLR4 signaling in vitro (34,35). Hence, these data collectively indicate that ER stress may underlie decreases in TLR2 and TLR4 signaling and affect immune function in patients with diabetes.

TLR3 signaling is different from the other TLR signaling pathway; for example, it is independent of MyD88. TLR2 and TLR4 are expressed on the cell surface, whereas TLR3 is expressed in intracellular compartments such as endosomes (13), and its ligands require internalization before signaling occurs. This suggests that disturbances in TLR3 signaling in diabetic monocytes may be due to reasons other than ER stress. Further investigations are needed to elucidate the detailed mechanisms of attenuated TLR signaling in monocytes from patients with diabetes.

ER stress has been shown to be a mainstay of the diabetic condition. Its pathologic importance in diabetes is especially important in pancreatic β-cells, in which glucose toxicity results in ER stress and insufficient insulin secretion (36–38). The current study suggests that monocytes are yet another population of cells vulnerable to hyperglycemia-induced ER stress and dysfunction. Nevertheless, the mechanisms that render pancreatic β-cells and monocytes vulnerable to ER stress in patients with diabetes remain uncertain.

Diabetes is considered a chronic inflammatory disease. Activated macrophages that produce proinflammatory cytokines such as TNF-α, IL-1β, and IL-6 are thought to contribute to insulin resistance in muscle and adipose tissues (39,40). Furthermore, the atherosclerotic complications in patients with diabetes have a basis in inflammation; local inflammatory foci in atherosclerotic lesions are commonly composed of foam cells derived from activated macrophages (41,42). Further studies are needed to determine whether different subpopulations of monocyte-derived cells, for example, systemically circulating and locally residing inflammatory cells, are susceptible to hyperglycemia-induced ER stress and dysfunction.

In conclusion, our findings show that $CD14^+$ monocytes are susceptible to ER stress–induced alterations in inflammatory signaling and apoptosis, which may play a role in the decreased immune function observed in patients with diabetes. Further investigations are needed to discern the mechanisms of diabetes-induced ER stress and perturbations in inflammatory signaling in $CD14^+$ monocytes.

ACKNOWLEDGMENTS

No potential conflicts of interest relevant to this article were reported.

We thank Dr. Iseki for valuable advice and critical comments on electron microscopic examination about ER of monocytes.

REFERENCES

1. Stumvoll M, Goldstein BJ, van Haeften TW. Type 2 diabetes: principles of pathogenesis and therapy. Lancet 2005;365:1333–1346
2. Zimmet P, Alberti KG, Shaw J. Global and societal implications of the diabetes epidemic. Nature 2001;414:782–787
3. Joshi N, Caputo GM, Weitekamp MR, Karchmer AW. Infections in patients with diabetes mellitus. N Engl J Med 1999;341:1906–1912
4. Shah BR, Hux JE. Quantifying the risk of infectious diseases for people with diabetes. Diabetes Care 2003;26:510–513
5. Finney SJ, Zekveld C, Elia A, Evans TW. Glucose control and mortality in critically ill patients. JAMA 2003;290:2041–2047
6. Dunn GP, Old LJ, Schreiber RD. The immunobiology of cancer immunosurveillance and immunoediting. Immunity 2004;21:137–148
7. Karin M, Lawrence T, Nizet V. Innate immunity gone awry: linking microbial infections to chronic inflammation and cancer. Cell 2006;124:823–835
8. Delamaire M, Maugendre D, Moreno M, Le Goff MC, Allannic H, Genetet B. Impaired leucocyte functions in diabetic patients. Diabet Med 1997;14:29–34
9. Geerlings SE, Hoepelman AI. Immune dysfunction in patients with diabetes mellitus (DM). FEMS Immunol Med Microbiol 1999;26:259–265
10. Katz S, Klein B, Elian I, Fishman P, Djaldetti M. Phagocytotic activity of monocytes from diabetic patients. Diabetes Care 1983;6:479–482
11. Geisler C, Almdal T, Bennedsen J, Rhodes JM, Klendorf K. Monocyte functions in diabetes mellitus. Acta Pathol Microbiol Immunol Scand C 1982;90:33–37
12. Takamura T, Honda M, Sakai Y, Ando H, Shimizu A, Ota T, Sakurai M, Misu H, Kurita S, Matsuzawa-Nagata N, Uchikata M, Nakamura S, Matoba R, Tanino M, Matsubara K, Kaneko S. Gene expression profiles in peripheral blood mononuclear cells reflect the pathophysiology of type 2 diabetes. Biochem Biophys Res Commun 2007;361:379–384
13. Akira S, Uematsu S, Takeuchi O. Pathogen recognition and innate immunity. Cell 2006;124:783–801
14. Pasare C, Medzhitov R. Toll-like receptors: linking innate and adaptive immunity. Microbes Infect 2004;6:1382–1387
15. Tateno M, Honda M, Kawamura T, Honda H, Kaneko S. Expression profiling of peripheral-blood mononuclear cells from patients with chronic hepatitis C undergoing interferon therapy. J Infect Dis 2007;195:255–267
16. Stuart LM, Ezekowitz RA. Phagocytosis and comparative innate immunity: learning on the fly. Nat Rev Immunol 2008;8:131–141
17. Thoma-Uszynski S, Stenger S, Takeuchi O, Ochoa MT, Engele M, Sieling PA, Barnes PF, Rollinghoff M, Bolcskei PL, Wagner M, Akira S, Norgard MV, Belisle JT, Godowski PJ, Bloom BR, Modlin RL. Induction of direct antimicrobial activity through mammalian toll-like receptors. Science 2001;291:1544–1547
18. Barton GM, Medzhitov R. Toll-like receptor signaling pathways. Science 2003;300:1524–1525
19. Sabroe I, Parker LC, Dower SK, Whyte MK. The role of TLR activation in inflammation. J Pathol 2008;214:126–135
20. Iwasaki A, Medzhitov R. Toll-like receptor control of the adaptive immune responses. Nat Immunol 2004;10:987–995
21. Ghanim H, Mohanty P, Deopurkar R, Sia CL, Korzeniewski K, Abuaysheh S, Chaudhuri A, Dandona P. Acute modulation of Toll-like receptors by insulin. Diabetes Care 2008;31:1827–1831

22. Dasu MR, Devaraj S, Zhao L, Hwang DH, Jialal I. High glucose induces toll-like receptor expression in human monocytes: mechanism of activation. Diabetes 2008;57:3090–3098
23. Desfaits AC, Serri O, Renier G. Normalization of plasma lipid peroxides, monocyte adhesion, and tumor necrosis factor-alpha production in NIDDM patients after gliclazide treatment. Diabetes Care 1998;21:487–493
24. Ohno Y, Aoki N, Nishimura A. In vitro production of interleukin-1, interleukin-6, and tumor necrosis factor-alpha in insulin-dependent diabetes mellitus. J Clin Endocrinol Metab 1993;77:1072–1077
25. Renier G, Mamputu JC, Serri O. Benefits of gliclazide in the atherosclerotic process: decrease in monocyte adhesion to endothelial cells. Metabolism 2003;52:13–18
26. Serbina NV, Jia T, Hohl TM, Pamer EG. Monocyte-mediated defense against microbial pathogens. Annu Rev Immunol 2008;26:421–452
27. Wahl LM, Wahl SM, Smythies LE, Smith PD. Isolation of human monocyte populations. Curr Protoc Immunol 2006;Chapter 7:Unit 7.6A
28. Ron D, Walter P. Signal integration in the endoplasmic reticulum unfolded protein response. Nat Rev Mol Cell Biol 2007;8:519–529
29. Xu C, Bailly-Maitre B, Reed JC. Endoplasmic reticulum stress: cell life and death decisions. J Clin Invest 2005;115:2656–2664
30. Bukau B, Weissman J, Horwich A. Molecular chaperones and protein quality control. Cell 2006;125:443–451
31. Wang XZ, Ron D. Stress-induced phosphorylation and activation of the transcription factor CHOP (GADD153) by p38 MAP Kinase. Science 1996;272:1347–1349
32. McCullough KD, Martindale JL, Klotz LO, Aw TY, Holbrook NJ. Gadd153 sensitizes cells to endoplasmic reticulum stress by down-regulating Bcl2 and perturbing the cellular redox state. Mol Cell Biol 2001;21:1249–1259
33. Kataoka H, Yasuda M, Iyori M, Kiura K, Narita M, Nakata T, Shibata K. Roles of N-linked glycans in the recognition of microbial lipopeptides and lipoproteins by TLR2. Cell Microbiol 2006;8:1199–1209
34. Ohnishi T, Muroi M, Tanamoto K. N-linked glycosylations at Asn(26) and Asn(114) of human MD-2 are required for toll-like receptor 4-mediated activation of NF-kappaB by lipopolysaccaharide. J Immunol 2001;167:3354–3359
35. Weber AN, Morse MA, Gay NJ. Four N-linked glycosylation sites in human toll-like receptor 2 cooperate to direct efficient biosynthesis and secretion. J Biol Chem 2004;279:34589–34594
36. Ozcan U, Cao Q, Yilmaz E, Lee AH, Iwakoshi NN, Ozdelen E, Tuncman G, Görgün C, Glimcher LH, Hotamisligil GS. Endoplasmic reticulum stress links obesity, insulin action, and type 2 diabetes. Science 2004;306:457–461
37. Oyadomari S, Takeda K, Takiguchi M, Gotoh T, Matsumoto M, Wada I, Akira S, Araki E, Mori M. Nitric oxide-induced apoptosis in pancreatic beta cells is mediated by the endoplasmic reticulum stress pathway. Proc Natl Acad Sci U S A 2001;98:10845–10850
38. Schenk S, Saberi M, Olefsky JM. Insulin sensitivity: modulation by nutrients and inflammation. J Clin Invest 2008;118:2992–3002
39. Kahn SE, Hull RL, Utzschneider KM. Mechanisms linking obesity to insulin resistance and type 2 diabetes. Nature 2006;444:840–846
40. Wellen KE, Hotamisligil GS. Inflammation, stress, and diabetes. J Clin Invest 2005;115:1111–1119
41. Brownlee M. Biochemistry and molecular cell biology of diabetic complications. Nature 2001;414:813–820
42. Liang CP, Han S, Senokuchi T, Tall AR. The macrophage at the crossroads of insulin resistance and atherosclerosis. Circ Res 2007;100:1546–1555

INTERNAL MEDICINE

□ EDITORIAL □

Abnormal Liver Function Tests and Metabolic Syndrome—Is Fatty Liver Related to Risks for Atherosclerosis beyond Obesity?

Masaru Sakurai[1], Toshinari Takamura[2], Katsuyuki Miura[3], Shuichi Kaneko[2] and Hideaki Nakagawa[1]

Key words: fatty liver, metabolic syndrome

(Inter Med 48: 1573-1574, 2009)
(DOI: 10.2169/internalmedicine.48.2517)

Oda and colleagues (1) reported that elevated liver enzymes, such as alanine aminotransferase (ALT) and gamma-glutamyltransferase (GGT), are related to metabolic syndrome (MetS) in Japanese men and women. One of the main causes of abnormal liver function is fatty liver disease. Recently, it was reported that non-alcoholic fatty liver disease (NAFLD) is related to cardiovascular disease (CVD) (2-5) and to most cardiovascular risk factors, including diabetes, hypertension, hyperlipidemia, and MetS (2, 5-7). Some of the suggested biological mechanisms linking NAFLD and accelerated atherosclerosis are insulin resistance, oxidative stress, inflammation, adiponectin and other adipocytokines, and abnormal lipoprotein metabolism (8, 9).

Insulin resistance and visceral adipose tissue are the two major risk factors underlying MetS, and play a pivotal role in the development of NAFLD and atherosclerosis. These confounding factors should be considered when evaluating the relationships among NAFLD, MetS, and atherosclerosis. Some prospective studies showed that increases in liver function parameters, such as GGT (2, 3) and ALT (4), are associated with the incidence of CVD events, even after adjusting for body mass index (BMI) and other components of MetS. In contrast, in an 11-year follow-up of Australians, Adams et al (6) showed that the presence of NAFLD did not increase the risk of MetS after adjusting for baseline waist circumference and other components of MetS. McKimmie et al (10) evaluated the association between hepatic steatosis and carotid atherosclerosis in the Diabetic Heart Study, and suggested that hepatic steatosis is unlikely a direct mediator of CVD. In other epidemiological studies that evaluated the association between NAFLD and MetS or CVD, the role of obesity was not evaluated fully, although most of those with NAFLD or elevated liver enzymes tended to have higher BMIs or waist circumferences (1, 5, 7). There is insufficient epidemiological evidence in clinical practice to determine whether NAFLD is related to MetS and CVD directly, beyond obesity and insulin resistance.

In Western countries, the prevalence of NAFLD is between 24 and 42% (11, 12), and NAFLD is widely reported to be the most common chronic liver condition. In Asian countries, NAFLD is assumed to be less common. However, the reported prevalence of NAFLD in Asian populations ranges from 5-40% and the increase in NAFLD is also an important problem in Asia (13). Recently, a prospective study in China showed that NAFLD was closely associated with the onset of metabolic disorders, even among non-obese subjects (14). Subsequently, data from lean NAFLD patients in Asia would provide insight into whether NAFLD increases the risk of MetS or CVD beyond obesity.

Patients with NAFLD are at higher risk for MetS and CVD, and thus should be monitored intensively to reduce the risk factors for atherosclerosis. However, further epidemiological studies are needed to evaluate whether the presence of NAFLD or elevated liver enzymes should be dealt with as a component of MetS, as is the case with other classical CVD risk factors.

[1]Department of Epidemiology and Public Health, Kanazawa Medical University, Ishikawa, [2]Department of Disease Control and Homeostasis, Kanazawa University Graduate School of Medical Science, Kanazawa and [3]Department of Health Science, Shiga University of Medical Science, Otsu

Received for publication May 27, 2009; Accepted for publication June 2, 2009

Correspondence to Dr. Masaru Sakurai, m-sakura@kanazawa-med.ac.jp